

The spin echo in systems with a coupled electron-nuclear precession

A. S. Borovik-Romanov, Yu. M. Bun'kov, B. S. Dumesh, M. I. Kurkin, M. P. Petrov,
and V. P. Chekmarev

Institute of Physical Problems, Academy of Sciences of the USSR; Institute of Nuclear Research, Academy of Sciences of the USSR; Institute of the Physics of Metals, Ural Scientific Center, Academy of Sciences of the USSR, Sverdlovsk; A. F. Ioffe Physicotechnical Institute, Academy of Sciences of the USSR, Leningrad
Usp. Fiz. Nauk **142**, 537-570 (April 1984)

TABLE OF CONTENTS

I. Introduction	235
II. Theoretical concepts.....	237
1. Basic aspects of NMR in magnetic crystals. 2. Dynamics of nuclear magnetization with a dynamic frequency shift in a transverse rf field. 3. Induction and echo. 4. Frequency-modulated echo.	
III. Experimental research	244
5. Measurement methods. 6. Magnetically ordered crystals which have been studied. 7. Free-induction signal. 8. Spin-echo signals. 9. Spin systems with a small dynamic NMR frequency shift. 10. Dynamic NMR frequency shift of nuclei in domain walls.	
IV. Conclusion.....	253
References.....	254

I. INTRODUCTION

Research on nuclear magnetic resonance (NMR) in condensed media began soon after Zavoiskii's discovery of an analogous resonance for electrons in paramagnetic salts.¹ This research was undertaken simultaneously by two groups: Purcell, Torrey, and Pound² and Bloch, Hansen, and Packard.³ The potentialities of the NMR method were increased substantially by Hahn's discovery⁴ of the spin echo, which has made it possible to study transient processes in spin systems.

Research on magnetic crystals represented a new stage in the development of the NMR method, since the magnetically ordered system of electron magnetic moments causes important changes in the behavior of nuclear spins. This research was begun by Poullis and Hardemann,⁵ who studied the NMR spectra and relaxation of hydrogen nuclei in $\text{CuCl}_2 \cdot 2\text{H}_2\text{O}$. A really comprehensive picture of NMR in magnetically ordered systems first emerged from studies by Gossard and Portis,⁶ who discovered the NMR in ferromagnetic iron and cobalt.

Subsequent research on NMR in magnetic crystals has yielded a great deal of information about the properties of magnetic materials and has contributed greatly to our understanding of NMR itself. The NMR method has yielded the most accurate measurements of the local magnetic field at nuclei and of the distribution of the spin density in paramagnets, and it has made it possible to study the temperature dependence of the magnetizations of sublattices in antiferromagnets and ferrites (including the dependence near phase-transition points), to study the magnetic structure of several complex compounds, to determine exchange integrals, to determine the effectiveness of certain relaxation mechanisms, to establish the existence of nuclear spin waves, etc.

The field of NMR has been enriched by such concepts as the gain effect, the indirect nucleus-nucleus interaction

(the Suhl-Nakamura interaction), and nuclear spin waves. New double resonances have been discovered: the nuclear-ferromagnetic and nuclear-antiferromagnetic resonances. Research on the nuclear acoustic resonance in antiferromagnets has recently been developing rapidly.

Many of these questions are of independent interest, and some have become the subjects of reviews and monographs.⁷⁻¹⁸

The present review is devoted to a new aspect of NMR in magnetic crystals. This new aspect stems from the strong nonlinear phenomena which come into play in the nuclear and electron spin subsystems at low temperatures (of the order of the temperature of liquid helium). In solving the problem of coupled electron-nuclear oscillations in this case we need to consider not only the effect of the hyperfine field on the nuclear spin subsystem but also the motion of the electron spin subsystem in the average field exerted by the precessing nuclei. In other words, the dynamics of the precession of the nuclear magnetization (\mathbf{m}) and the electron magnetization (\mathbf{M}) (i.e., the magnetic moments per unit volume) can be described in a simplified way in this case in terms of the oscillations of two interacting oscillators—these oscillators being the transverse components of the vectors \mathbf{m} and \mathbf{M} . As in a system of interacting oscillators of any sort, there is a repulsion of the frequencies of combined oscillations in comparison with the original (unshifted) resonant frequencies of each of the individual subsystems. This so-called dynamic frequency shift¹⁹ is found to depend on the angle (α) by which the magnetization \mathbf{m} deviates from its equilibrium orientation (i.e., on the oscillation amplitude of \mathbf{m}):

$$\omega_{n0} - \omega_n = \omega_p \cos \alpha, \quad (1)$$

where ω_n and ω_{n0} are respectively the shifted and unshifted NMR frequencies, and ω_p is the parameter of the dynamic

frequency shift.¹⁾ It is this dependence of the NMR frequency on the oscillation amplitude which gives rise to the non-linearity whose consequences are the subject of this review.

The parameter ω_p in (1) depends strongly on the type of magnetic order, reaching its highest values for easy-plane and cubic antiferromagnets (MnCO_3 , CsMnF_3 , and RbMnF_3 , for example²⁰). In the experiments which we will be discussing below the value of $\omega_p/2\pi$ is usually of the order of 10–100 MHz at the frequency of $\omega_{n0}/2\pi \sim 600$ MHz.

A distinctive feature of this problem is that the electron spin system is ordered, while the nuclear spin system is paramagnetic.

In a real crystal there is a spread in the values of the hyperfine field at adjacent nuclei, called "microinhomogeneous broadening." Because of the particular nature of the problem, the point in which we are interested here is the microinhomogeneous broadening $\delta\omega$ within the correlation radius of the oscillations of the electron spins (which is roughly equal to the thickness of a domain wall). In studying oscillations near the unshifted NMR frequency ω_{n0} in this case we can distinguish between two fundamentally different situations. If the calculated dynamic frequency shift²⁾ is such that the condition $\omega_p \ll \delta\omega$ holds then the microinhomogeneous broadening will suppress the dynamic frequency shift. In this case the presence of an ordered electron system leads to only the well-known features of NMR in magnetic crystals (Section 1). If the condition $\omega_p \gg \delta\omega$ holds, on the other hand, the microinhomogeneous broadening is suppressed. This means that the precession of the ordered electron spin system causes the nuclear spins to precess coherently in the correlation region. The coherence radius is of the order of 10^2 – 10^4 atomic spacings. The precession frequency ω_n corresponds to (1). The quasinuclear oscillation mode has several properties which we would usually associate with ordered systems (nuclear spin waves, several relaxation processes, etc.). In a rigorous analysis, therefore, a single oscillator in a situation with a coupled nuclear-electron precession is a macroscopic set of nuclear and electron spins in the correlation region of the oscillations of the electron spin system. Except in Sections 10 and 11, we will confine this review to systems with a large dynamic NMR frequency shift and a steady-state coupled electron-nuclear precession.

The NMR spectra and the spectra of ferromagnetic and antiferromagnetic resonances under conditions with a dynamic frequency shift have been the subject of theoretical and experimental research for several years. The experimen-

tal work has been carried out by so-called continuous methods.^{9,20,21} The pulsed excitation of oscillations and the echo effect went without study for a rather long time, partly due to the doubt that it would be possible at all to observe an echo signal in systems with a nonlinearity of this type.¹⁹ At first glance it would seem that the dynamic frequency shift would make it impossible to observe intense echo signals, since, in particular, a deviation from equilibrium would cause a mismatch between the precession frequency of the nuclear magnetization and the frequency of the external agent; this mismatch would make it impossible to deflect the magnetization through an angle large enough for observation of an intense echo signal.

Although these circumstances do impose certain restrictions on the observation conditions, yet it turns out that they not only do not rule out the possible formation of echo signals but in fact give rise to a new mechanism for the formation of a spin echo: the so-called frequency-modulation mechanism. This mechanism can be summarized by saying that two rf pulses give rise to a periodic modulation of the shape function of the NMR line with a period $1/\tau_{12}$ (τ_{12} is the time interval between the first and second rf pulses). After this time the system of nuclear spins can be thought of roughly as a set of oscillators whose frequencies differ by a discrete value of $1/\tau_{12}$. When such a system is excited, beats naturally appear at time intervals τ_{12} , and these beats constitute the echo signals.

The basic distinguishing feature of the frequency-modulation echo is that its intensity reaches a maximum (of the order of the intensity of the induction signal) when the angle (α) by which the nuclear magnetization deviates from its equilibrium direction is small. For maximum phasing of a spin system with a dynamic frequency shift at the time in which the echo signal is formed, the magnitude of the frequency modulation, $\Delta\omega_p^1 \approx \omega_p \alpha^2$, multiplied by the delay time τ_{12} must be of the order of π . Hence we have $\alpha \approx \sqrt{\pi/\omega_p \tau_{12}}$. The frequency ω_p is usually in the range 10–100 MHz, while τ_{12} is in the range 10–100 μs , so that we have $\alpha \sim 0.1$ – 0.01 rad.

Another distinctive feature of the frequency-modulation echo is the nonmonotonic dependence of its intensity on the delay time. The intensity of the echo signal should increase with increasing delay time while this time is short, at least at small amplitudes of the exciting pulses. This conclusion follows from the circumstance that by the time the echo signal is formed the frequency modulation must cause a sufficient change in the phase distribution of the spins. For long delays, relaxation processes reduce the intensity of the echo signal.

Finally, the time at which the frequency-modulation echo appears may be shifted from the time $2\tau_{12}$. The reason for this shift is that the rf pulses not only use a periodic modulation but also cause some deformation of the shape of the NMR line, which changes the average distance between the oscillators.

The possibility of producing intense frequency-modulation echo signals at small spin deviation angles makes it possible to observe echo signals also in the case of a "nonresonant" excitation, with intense rf pulses applied at frequencies

¹⁾This repulsion causes a frequency shift of the same magnitude but of opposite sign on the electron wave branch. The relative shift $\Delta\omega_e/\omega_e$, however (ω_e is the frequency of the electron resonance, and $\Delta\omega_e$ is the dynamic frequency shift for the electron system), is generally much smaller than for the nuclear system (since $\omega_e > \omega_n$) and comparable to the line width of the antiferromagnetic resonance. The dynamic frequency shift on the electron branch is furthermore masked by the effect of the static (average) hyperfine field which is exerted on the electron system by the nuclear magnetization. The static effect of the nuclear magnetization on the antiferromagnetic resonance frequency may be quite important. It is this effect which allowed Heeger and Portis²¹ to discover the double nuclear antiferromagnetic resonance in KMnF_3 .

²⁾The dynamic frequency shift ω_p is calculated in the homogeneous approximation. See Section 7 for expressions for ω_p in the case of easy-plane antiferromagnetic materials.

different from the NMR frequency. At the same time it became possible to understand also the mechanism for the formation of the so-called single-pulse echo which is observed in the case of nonresonant excitation. The magnitude of the single-pulse echo in nuclear systems with a dynamic frequency shift is much higher than in ordinary nuclear spin systems.

The parametric echo^{17,22} due to the existence of coupled oscillations of an electron-nuclear system was an essentially novel effect. However, parametric effects are not discussed in this review. We will simply report some results on the dynamics of a nuclear system with a dynamic frequency shift which have been obtained by the parametric-echo method.

II. THEORETICAL CONCEPTS

1. Basic aspects of NMR in magnetic crystals

The factor which primarily governs the behavior of the nuclear spin system in a magnetic crystal is the electron-nuclear hyperfine interaction. However, the coordinated motion of the electron magnetic moments over macroscopically large distances which is characteristic of a magnetically ordered state makes all the hyperfine effects quite different from those in paramagnetic substances in which the paramagnetic ions are impurities. In this case, instead of the discrete spectrum of the atomic magnetic moment in an impurity paramagnetic material²³ deal with a continuous spectrum of magnetization oscillations of macroscopically large volumes of the medium (the spin-wave spectrum²⁴). As a result, both the electron magnetization $\mathbf{M}(r)$ and the nuclear magnetization $\mathbf{m}(r)$ can be treated at a purely classical level, except in rare cases (involving relaxation processes and quadrupole effects). We can thus write the hyperfine-interaction energy as⁹

$$\hat{\mathcal{H}}_{\text{hf}}(r) = A\mathbf{M}(r) \cdot \mathbf{m}(r), \quad (2)$$

where the hyperfine-interaction constant A is assumed to be purely isotropic, since essentially all the experiments which we will discuss in this review have been carried out with the nuclei of the magnetic ions in the S state (Mn^{2+} , Fe^{3+}), and the anisotropy of the surroundings is not important (r is a radius vector).

It can be seen from (2) that the effect of $\hat{\mathcal{H}}_{\text{hf}}$ on the vector \mathbf{m} may be regarded as the effect of a magnetic field

$$\mathbf{H}_n = -A\mathbf{M}(r), \quad (3)$$

which is called the "hyperfine field." Since the thermal oscillations of the atomic magnetic moments in a magnetically ordered state are small at $T \ll T_c$ (T_c is the ordering temperature), so that the values of $\mathbf{M}(r)$ are near their maximum, we see that the fields $\mathbf{H}_n(r)$ in (3) reach high levels, of the order of 10^5 – 10^6 Oe, so that they are governing with respect to the nuclear spin system. In the paramagnetic region, where \mathbf{M} is much smaller than its maximum value, the local magnetic fields observed at nuclei are weak.

In addition to \mathbf{H}_n in (3) it is convenient to introduce the hyperfine field

$$\mathbf{H}_{\text{en}}(r) = -A\mathbf{m}(r), \quad (4)$$

which is exerted by the nuclear spins on the electrons. The

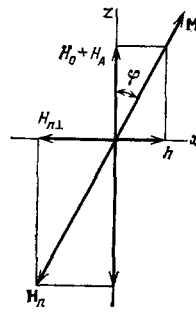


FIG. 1. Diagram illustrating the determination of the gain of the rf field.

field \mathbf{H}_{en} is much weaker than \mathbf{H}_n , and even for Mn^{55} nuclei, with a large spin ($I = 5/2$), at a 100% concentration of the isotope, and with a comparatively large gyromagnetic ratio, we find that H_{en} is of the order of 1 Oe at $T \sim 1$ K. Although this field is far weaker than the fields which we mentioned above, and which are responsible for the magnetic ordering, it may not be weak in comparison with the magnetic-anisotropy fields.³⁾ It is this case which is the most interesting from our standpoint. The effect of the static part of the field \mathbf{H}_{en} , which is related to the average value of \mathbf{m} , on the electron system is equivalent to some additional anisotropy field; there is accordingly a static frequency shift of the ferromagnetic or antiferromagnetic resonance associated with this field. This shift is studied by the methods of double electron-nuclear resonance.

The governing role played by the hyperfine interaction for the nuclear spin system intensifies the observed NMR signal and the external rf field at the nuclei.

This amplification can be explained most simply in the case of a ferromagnetic material which is magnetized to saturation in an external field \mathbf{H}_0 (Fig. 1). We assume that the field \mathbf{H}_0 is directed along the anisotropy field \mathbf{H}_A . An alternating field h is applied in the plane perpendicular to \mathbf{H}_0 and deflects the electron moment through an angle

$$\varphi = \frac{h}{H_0 + H_A}. \quad (5)$$

Correspondingly, a perpendicular oscillatory component of the field \mathbf{H}_n arises:

$$H_{n\perp} = H_n \frac{h}{H_0 + H_A} = \eta h. \quad (6)$$

It is the parameter

$$\eta = \frac{H_n}{H_0 + H_A} \quad (7)$$

which is the effective "gain" of the rf field. This gain is conveniently expressed in terms of the susceptibility of the sample:

$$\eta = A\chi. \quad (8)$$

In this case expressions (7) and (8) are identical since

³⁾The "anisotropy field" in a magnetic crystal is the effective magnetic field which characterizes the energy required to deflect the magnetic moment of the sample from its stable equilibrium direction along the corresponding crystal axis.

$$\chi = \frac{M}{H_0 + H_A}. \quad (9)$$

From (8) and (4) we see that the NMR intensity is also increased by a factor of η since an emf is induced in the receiver not only directly by the transverse component of the nuclear moment, m_1 , but also by the field H_{en} : $M_1 = \chi H_{en1} = -\chi A m_1 = -\eta m_1$. These simple arguments reflect the circumstance that the nuclear resonance in a magnetic crystal is actually not a "purely" nuclear resonance. It is a resonance of an electron-nuclear system at the NMR frequency. The gain values for magnetized ferromagnetic materials and ferrites can be of the order of 10^2 – 10^3 . A similar amplification occurs in antiferromagnetic materials.⁴⁾ The derivation of the expressions for antiferromagnetic materials is not as graphic, but we might note that if H_0 is sufficiently large in comparison with the parameter $\sqrt{H_E H_A}$ we would have $\eta \sim H_n/H_0$; here H_E is the effective exchange field, which describes the exchange interaction.

The amplification effects are only one manifestation of the interaction of the oscillations of the electron and nuclear magnetizations. Other effects associated with this interaction, as we mentioned in the Introduction, are the dynamic frequency shifts of these oscillations. To find expressions for these shifts we again use expressions (3) and (4) for the fields H_n and H_{en} ; we substitute these expressions into the equations of motion for the magnetic moments:

$$\begin{aligned} \dot{\mathbf{m}} &= \gamma [\mathbf{m}, \mathbf{H}_n], \\ \dot{\mathbf{M}} &= \gamma_e [\mathbf{M}, \mathbf{H}_e + \mathbf{H}_{en}], \end{aligned} \quad (10)$$

where γ and γ_e are the gyromagnetic ratios of the nuclei and electrons, and the effective magnetic field H_e is due to the interactions within the electron subsystem (the exchange, dipole, spin-orbit, etc., interactions).

Using expression (3) for the field H_n , we can write Eq. (10) for the vector \mathbf{m} in component form as follows:

$$\begin{cases} \dot{m}_x = A\gamma (M_z m_y - M_y m_z), \\ \dot{m}_y = A\gamma (M_x m_z - M_z m_x), \\ \dot{m}_z = A\gamma (M_y m_x - M_x m_y), \end{cases} \quad (11)$$

where the components $M_{x,y,z}$ are the solutions of the second of Eqs. (10).

The problem of finding the components of the vector \mathbf{M} simplifies greatly if the deflections of this vector caused by the field H_{en} are small. In this case, these deflections can be expressed in terms of the components of the magnetic susceptibility tensor $\chi^{\alpha\beta}$, which is well known.²⁴

As an example we again consider the case of a ferromagnetic material adopting a coordinate system with z axis along

⁴⁾We recall that in the simplest case an antiferromagnetic substance is a magnetically ordered medium with a zero resultant moment. In this case the magnetic structure may be represented as two or more magnetic sublattices with the magnetic moment of a sublattice being equal in magnitude but opposite in direction to the magnetic moment of another, so that the crystal as a whole does not have a spontaneous moment. In more complicated cases, e.g., in so-called weak ferromagnetic materials, the magnetic moments of the sublattices are not directed strictly opposite to each other, so that there is a small resultant moment. The effective magnetic field responsible for the noncollinear arrangement of sublattice magnetizations is called the "Dzyaloshinskii field,"²⁵ H_D .

the equilibrium orientation of \mathbf{M} . Since the effect of the field H_{en} in this case is qualitatively the same as the effect of an rf field, and under the condition $\omega_e \gg \omega_i$, we can easily find the transverse components of the vector produced by the field H_{en} , working from Fig. 1:

$$\left. \begin{aligned} M_z &= M_0, \\ M_x &= \frac{M_0}{H_0 + H_A} A m_x = \eta m_x, \\ M_y &= \eta m_y. \end{aligned} \right\} \quad (12)$$

Substituting these expressions into (11), we find the system of equations

$$\left. \begin{aligned} \dot{m}_z &= 0, \\ \dot{m}_x &= \left(\omega_{n0} - \omega_p \frac{m_z}{m_0} \right) m_y, \\ \dot{m}_y &= - \left(\omega_{n0} - \omega_p \frac{m_z}{m_0} \right) m_x, \end{aligned} \right\} \quad (13)$$

where the quantities

$$\omega_{n0} = A\gamma M_0 = \gamma H_n, \quad \omega_p = A\gamma \eta m_0 = \omega_{n0} \eta \frac{m_0}{M_0} \quad (14)$$

are the unshifted NMR frequency and the dynamic frequency shift. Equations (13) with $m_z = \text{const}$ describe a circular precession of the vector \mathbf{m} around the field H_n at a frequency (Fig. 2a)

$$\omega_n = \omega_{n0} - \omega_p \frac{m_z}{m_0} = \omega_{n0} - \omega_p \cos \alpha. \quad (15)$$

In this example the ferromagnetic material is isotropic in the (x, y) plane. If there were an anisotropy in the (x, y) plane the gain values along the x and y axes (η^{xx} and η^{yy}) would be different, and the precession of the vector \mathbf{m} would change from circular to elliptical. This change can be ignored, however, everywhere except in parametric effects,^{17,22} with which we are not concerned in the present review.

It is a far more complicated matter to calculate the dynamic frequency shift ω_p for antiferromagnetic rather than for ferromagnetic materials, but the simple relation $\omega_n \omega_e = \omega_{n0} \omega_{e0}$ holds quite accurately for the corresponding frequencies; here ω_{n0} and ω_{e0} are the unperturbed NMR

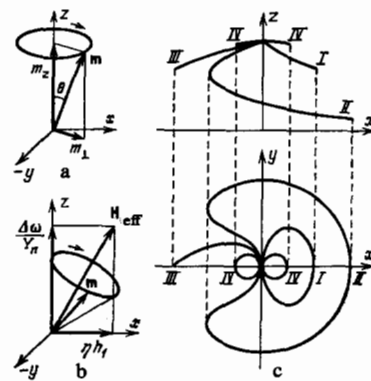


FIG. 2. Motion of the nuclear magnetization vector \mathbf{m} in various cases.¹⁵ a: In the absence of an rf field, $\mathbf{h}_1 = 0$. b: $\mathbf{h}_1 \perp z$. c: Various types of trajectories of \mathbf{m} in the case of a dynamic shift of the NMR frequency with $\mathbf{h}_1 \perp z$ and an initial orientation $\mathbf{m} \parallel z$. I— $\Delta\omega = 0$; II— $0 > \Delta\omega > -Q$; III— $\Delta\omega = -Q$; IV— $|\Delta\omega| > Q$, $Q = 3 \cdot 2^{-2/3} \omega_p^{1/3} \omega_1^{2/3}$.

and antiferromagnetic-resonance frequencies, and ω_n and ω_e are the corresponding frequencies when in (4) we take into account the field H_{en} exerted by the nuclei. The dynamic frequency shift in the case $\omega_e \gg \omega_n$ can be estimated from the following expressions:

a)

$$\omega_p = \omega_{n0} \frac{H_E H_n}{2H_0^2} \frac{m_0}{M_0} \quad (16)$$

for an easy-plane antiferromagnetic substance in a magnetic field $H_0 \perp c$ (c is the special crystal axis⁹), where M_0 and m_0 are the equilibrium electron and nuclear magnetizations of one magnetic sublattice;

b)

$$\omega_p = \omega_{n0} \frac{H_E H_n}{2(H_0^2 - H_c^2)} \frac{m_0}{M_0} \quad (17)$$

for a cubic antiferromagnetic substance in a magnetic field $H_0 > H_c$ ($H_c = H_E H_A$ is the critical anisotropy field or the flipping field); and

c)

$$\omega_p = \omega_{n0} \frac{H_E H_n}{2H_0(H_0 + H_D)} \frac{m_0}{M_0}, \quad (18)$$

for a weak easy-plane ferromagnetic substance in a magnetic field $H_0 \perp c$, where H_D is the Dzyaloshinskii field.

The dynamic frequency shift could also be interpreted in terms of the Suhl-Nakamura interaction.²⁶ This is an interaction of the nuclear moments through the ordered electron spin system. If a nuclear moment at the point j is deflected from its equilibrium position then the hyperfine interaction will also cause some deviation from equilibrium of the electron moment at the given atom. The resulting perturbation in the magnetically ordered electron system does not remain localized but instead propagates throughout the crystal, and the nuclear moments of other atoms (e.g., that of an atom at the point i) is affected by electron oscillations whose source is the nuclear spin at point j . The nuclear spins thus interact through electron spin waves. In practice this interaction occurs over distances shorter than some characteristic correlation radius in the electron system, which is 10^3 – 10^4 atomic spacings for antiferromagnetic materials with a slight anisotropy. The Hamiltonian of the Suhl-Nakamura interaction is

$$\hat{\mathcal{H}} = \sum_{i \neq j} u_{ij} (\hat{m}_{xi} \hat{m}_{xj} + \hat{m}_{yi} \hat{m}_{yj}), \quad (19)$$

where the operators $\hat{m}_{x,y,i,j}$ represent the electron spins at lattice sites i and j , and the interaction parameter u_{ij} depends on the properties of the electron system and is quadratic in the hyperfine interaction constant. The Suhl-Nakamura interaction is stronger in magnitude than the well-known dipole-dipole interaction between nuclear magnetic moments. Because of the partially collectivized nature of the nuclear spins (due to the Suhl-Nakamura interaction), the frequency of the homogeneous precession of the nuclear magnetization as a whole differs from the precession frequency for nuclear spins which are not interacting with each other. It is this frequency difference which represents the dynamic frequency shift.

The motion of the nuclear moments may also be inhomogeneous, in which case the motion can be described as

nuclear spin waves with a distinctive dispersion law.¹⁸ In this case the oscillation frequency depends on the wave vector, and the entire spectrum of nuclear spin waves lies between the homogeneous precession frequency and the frequency of the nuclear spins which are not interacting with each other. The Suhl-Nakamura interaction acquires an important feature for samples (usually antiferromagnetic) in which the magnetic susceptibility of the sample is anisotropic in the rotation plane of the nuclear magnetization (the x, y plane). The Suhl-Nakamura interaction then has two components: a secular component, i.e., one which commutes with the m_z component, and a nonsecular component, i.e., one which does not commute with the m_z component. The dynamic frequency shift is caused by the secular component, while the nonsecular component, which oscillates during the rotation of the nuclear magnetization, can give rise to parametric effects.^{17,22}

2. Dynamics of nuclear magnetization with a dynamic frequency shift in a transverse rf field

As usual, it is more convenient to use a coordinate system which is rotating at a frequency ω to describe the motion of nuclear moments in a linearly polarized transverse rf field,

$$\mathbf{h}_\perp(t) = 2\mathbf{h}_1 \cos \omega t, \quad \mathbf{h}_1 \perp H_0. \quad (20)$$

In this case the resonant component of the alternating field (i.e., the circularly polarized component, which is rotating along with the new coordinate system) is independent of the time. In ordinary spin systems the resonant frequency does not depend on m_z , so that the quantity $\Delta\omega = \omega_n - \omega$ is constant in the rotating coordinate system. The motion of the vector \mathbf{m} is a precession around the direction of the effective field H_{eff} , which has the following components in the rotating coordinate system (Fig. 2b):

$$H_{\text{eff}z} = \frac{\Delta\omega}{\gamma}, \quad H_{\text{eff}x} = \eta h_1. \quad (21)$$

The precession frequency is $\Omega = \gamma H_{\text{eff}}$.

In systems with a dynamic frequency shift a change in the component m_z leads to a change in the frequency difference $\Delta\omega$, and as a result the field H_{eff} in (21) changes in both magnitude and direction. The motion of \mathbf{m} becomes nonuniform, and the tip of the vector \mathbf{m} traces out a rather fanciful trajectory. To calculate the trajectories we can use Eqs. (13) in a rotating coordinate system, taking the field h_1 into account. We then have

$$\left. \begin{aligned} \dot{m}_x &= \Delta\omega (m_z) m_y, \\ \dot{m}_y &= -\Delta\omega (m_z) m_x + \omega_1 m_z, \\ \dot{m}_z &= -\omega_1 m_y, \end{aligned} \right\} \quad (22)$$

where

$$\omega_1 = \gamma h_1 \eta, \quad (23)$$

and ηh_1 is the amplitude of the rf field with allowance for the amplification, and

$$\Delta\omega (m_z) = \omega_n (m_z) - \omega = \omega_{n0} - \omega - \omega_p \frac{m_z}{m_0}. \quad (24)$$

Here $\Delta\omega (m_z)$ is the frequency of the free (if $\omega_1 = 0$) precession of \mathbf{m} in the rotating coordinate system.

Figure 2c shows some new types of trajectories calculated from (22). In particular, there are some unclosed trajectories with a stopping point at which $\mathbf{m} \parallel \mathbf{H}_{\text{eff}}$ and thus $\dot{\mathbf{m}} = \dot{m} = 0$ (curve III in Fig. 2c). Various aspects of the behavior of \mathbf{m} under conditions with a dynamic frequency shift were studied in Refs. 27–29. We will not go into these aspects in detail here, since it is difficult to study experimentally the details of the motion of \mathbf{m} along various trajectories because of the rather large inhomogeneous line broadening, i.e., the spread of the frequencies ω_{n0} and ω_p , which prevails in real samples.⁵⁾ We can ignore these inhomogeneities only if they are far smaller than $\omega_1 = \gamma\eta h_1$ in (23); i.e., the rf fields must have a rather large amplitude, and this requirement poses technical difficulties. Interestingly, a characteristic parameter

$$\delta_0 = \omega_p^{1/3} \omega_1^{2/3}, \quad (25)$$

arises in the theory of the dynamics of a nuclear system; this parameter can be used to find the conditions under which we can ignore the nonlinearity of the trajectories, i.e., ignore the change in the dynamic frequency shift during the excitation pulse. This is the case for a large frequency difference $\Delta\omega \gg \delta_0$ or a short pulse $\tau \ll 1/\delta_0$. Under these conditions, the motion of the nuclear magnetization during the rf pulses can be described in the same way as in the absence of dynamic frequency shift.

3. Induction and echo

The induction and echo signals are the response of the nuclear system to a pulsed perturbation (there may be one or several pulses). Induction signals are observed immediately after the exciting pulses, while the time at which the echo signals are observed is determined primarily by the time intervals between the excitation pulses. For example, the time at which the simplest two-pulse Hahn echo is observed is $t = 2\tau_{12}$, where τ_{12} is the time interval between the exciting pulses. For small perturbation amplitudes, for which the deflection angles are small ($m_{\perp} \ll m_z$), the induction is a linear response of the nuclear spins and is proportional to the amplitude of the perturbing pulse, while the echo signal is a nonlinear response of the nuclear system, proportional to the product of the amplitudes of the exciting pulses (or proportional to a product of these amplitudes raised to a power higher than the first). There is also a so-called single-pulse echo, which is formed from a single exciting pulse and which is generally proportional to the cube of its intensity. The single-pulse echo is usually observed after a time roughly equal to the length of the exciting pulse, after it has ended. We will first take up the induction and echo without a dynamic frequency shift.

In analyzing the induction and the echo we must take into account the inhomogeneous broadening of the NMR lines. In magnetic media this broadening is usually caused by the random variations in the local magnetic fields at the nuclei or by the inhomogeneous distribution of the electron magnetic moments in the sample due to a domain structure.

⁵⁾The only way to obtain direct experimental information on the motion of the magnetization is to use the parametric-echo method,^{17,22} scanning the NMR line which is excited.

Let us assume that the function $g(\Delta\omega)$ describes the shape of the NMR line and, as usual, is normalized:

$$\int g(\Delta\omega) d\Delta\omega = 1. \quad (26)$$

To pursue this analysis it is convenient to use the concept of an isochromatic grouping, i.e., a macroscopic nuclear moment formed by a group of spins:

$$m(\Delta\omega) = m_0 g(\Delta\omega) \delta\Delta\omega, \quad (27)$$

where the interval $\delta\Delta\omega$ is understood to be small enough that we may ignore the difference between the NMR frequencies of the spins in an individual isochromatic grouping ($\delta\Delta\omega T_1 \ll 1$) over the time (t_0) in which we are interested, which is of the order of several times T_1 . Here T_1 is the longitudinal spin relaxation time. On the other hand, this interval $\delta\Delta\omega$ must be large enough that $m(\Delta\omega)$ can be treated macroscopically.

Let us assume that a pulse of an alternating magnetic field of amplitude h_1 is applied along the x axis to the sample. The alternating field $h_1(t)$, acting for a short time τ_1 , then causes a rotation of the nuclear magnetization and gives rise to a transverse projection of the isochromatic grouping onto the y axis (Fig. 3a):

$$m_y(\Delta\omega) = m(\Delta\omega) \sin \alpha = m(\Delta\omega) \gamma\eta h_1 \tau_1, \quad (28)$$

where α is the angle through which the magnetization is deflected from the z axis.

We restrict the discussion to the case in which the time interval between the pulses, τ_{12} , is much shorter than the longitudinal relaxation times T_1 and T_2 , and the deflection angles α are much smaller than $\pi/2$.

Because of the change in the phase of the isochromatic grouping due to its rotation in the transverse plane, the transverse component of one isochromatic grouping at a time t after the end of the pulse is described by

$$m_{\perp}(\Delta\omega, t) = m(\Delta\omega) \alpha e^{-i\Delta\omega t}, \quad (29)$$

where $t = 0$ is the time in which the pulse is turned off, and $m_{\perp}(\Delta\omega, t) = m_y(\Delta\omega, t) - im_x(\Delta\omega, t)$. The total transverse magnetization is found by summing the magnetizations of the various isochromatic groupings:

$$m_{\perp}(t) = m_0 \alpha \int g(\Delta\omega) e^{-i\Delta\omega t} d\Delta\omega = m_0 \alpha F(t). \quad (30)$$

The emf induced in the receiving coil by the rotating moment $m_{\perp}(t)$ is a free-induction signal. We see from (30) that $m_{\perp}(t)$ and thus the induction signal are proportional to the Fourier transform of the NMR line, $F(t)$. For example, in the simple case in which the line has a Lorentzian shape,

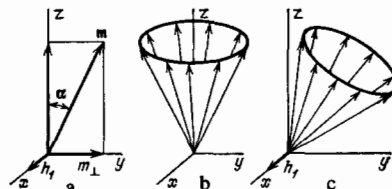


FIG. 3. Distribution of the vectors $\mathbf{m}(\Delta\omega)$ after the first rf pulse (a), at a time $t > T_2$ after this pulse (b), and after the second rf pulse (c).

$$g(\Delta\omega) = \frac{1}{\pi} \frac{1/T_2^*}{(\Delta\omega - \Delta\omega_0)^2 + (1/T_2^*)^2},$$

we would have

$$F(t) = e^{-t/T_2^*}, \quad (31)$$

where $\Delta\omega_0$ is the frequency difference between the center of the NMR line and the frequency of the alternating external field, and $1/T_2^*$ is a measure of the width of the NMR line. The induction signal is proportional to the time derivative of the nuclear moment in the laboratory coordinate system. The amplitude of the induction signal in the case $\Delta\omega \gg 1/T_2^*$ has a time dependence

$$U_v = U_0 \int g(\Delta\omega) e^{-i\Delta\omega t} d\Delta\omega = U_0 e^{-t/T_2^*}, \quad (32)$$

where $U_0 = c\omega_n \eta m_1(t=0)$, and the coefficient c reflects the technical characteristics of the receiver circuit (the quality factor, the filling factor, etc.) and a possible renormalization of the nuclear magnetization due to the multisublattice structure of the samples. The parameter $1/T_2^*$ is also a measure of the rate at which the transverse moment $m_1(t)$ decays into a fan of distinct isochromatic groupings (Fig. 3b). This decay of $m_1(t)$ into a fan occurs because each isochromatic grouping has its own rotation frequency. After a time interval T_2^* the nuclear magnetization is thus a cone formed by the set of isochromatic groupings rotated around the z axis (Fig. 3b). In the derivation of Eqs. (28)–(30) it was assumed that the pulse length satisfies $\tau_1 \ll T_2^*$.

We turn now to the dynamics of the nuclear magnetization and the formation of an echo when a sample is acted upon by two pulses. As before, we restrict the discussion to the case in which the time interval between the pulses is much longer than the relaxation times.

There is a well-known qualitative model which explains the appearance of the Hahn echo,⁴ for example, for a 90° , 180° pulse pair, i.e., for the case in which the first pulse rotates the magnetization by 90° and the second by 180° . After the first pulse (the alternating field is applied along the x axis) the nuclear magnetization has been rotated away from its equilibrium position (along the z axis) toward the y axis, and it spreads out into a fan of distinct isochromatic groupings in the x, y plane. The second rf pulse (also applied along the x axis, at a time τ_{12} after the first pulse) does not affect the m_x components of the isochromatic groupings, but it does reverse the direction of the m_y components; the effect corresponds to a phase inversion, i.e., a change in the sign of the phase of the isochromatic groupings from $\Delta\omega\tau_{12}$ to $-\Delta\omega\tau_{12}$.

The subsequent motion of the isochromatic groupings after the second pulse is the same as that after the first, so that the phase difference which builds up between the isochromatic groupings over the time interval τ_{12} , taken with the opposite sign, is cancelled by a new phase shift after the second pulse. As a result, by a time $t = 2\tau_{12}$ after the first pulse all the isochromatic groupings have the same phase. At this time a resultant magnetization therefore arises and gives rise to an emission, which is called the echo signal, in the laboratory coordinate system.

Let us examine this mechanism more carefully; for the

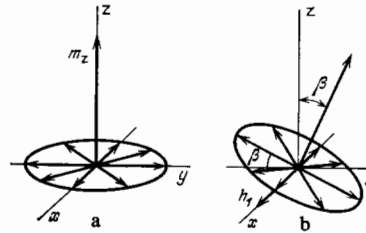


FIG. 4.

time being we will ignore the dynamic frequency shift. As for the induction signal, we consider small deflection angles. After the first magnetization pulse the isochromatic groupings thus form a cone (Fig. 3b). The second pulse, of length τ_2 , rotates this cone through a small angle $\beta = \gamma\eta h_1\tau_2$ away from the z axis (Fig. 3c). Assuming that the deflection angles are small, we will ignore the change in the longitudinal component m_z . At a time $t > \tau_{12}$ after the second pulse we can then write the following expression for the component $m_\perp(\Delta\omega, t)$ in the linear approximation in the angles α and β :

$$m_\perp(\Delta\omega, t) = m(\Delta\omega)\alpha e^{-i\Delta\omega t} + m(\Delta\omega)\beta e^{-i\Delta\omega(t-\tau_{12})}. \quad (33)$$

Expression (33) describes the induction signals after the first and second pulses, respectively. To find the Hahn-echo signal we must take into account the circumstance that the second exciting pulse acts nonuniformly on that system of transverse components of the nuclear magnetization which is created by the first pulse. In this case we can ignore the second term in (33).

In this case the effect of the second pulse reduces to rotating the fan of isochromatic groupings (29), which have been put out of phase, around the x axis (Fig. 4). We see that the isochromatic groupings which were directed along the x axis when the second pulse was applied [those groupings have frequencies $\Delta\omega = [(\pi/2) + n\pi]/\tau_{12}$] do not change direction, while the isochromatic groupings which are directed along the y axis ($\Delta\omega = n\pi/\tau_{12}$) are rotated through the maximum angle β . It is this nonuniformity of the effect of the second pulse which gives rise to the Hahn-echo signal.

The rotation of the fan of isochromatic groupings (29), which have been put out of phase, is described mathematically by

$$\begin{aligned} m_x(\Delta\omega, \tau_{12}) &= m(\Delta\omega)\alpha \sin \Delta\omega\tau_{12}, \\ m_y(\Delta\omega, \tau_{12}) &= m(\Delta\omega)\alpha(1 - \beta^2/2) \cos \Delta\omega\tau_{12} \end{aligned} \quad (34)$$

or, in terms of the complex notation (29),

$$\begin{aligned} m_\perp(\Delta\omega, \tau_{12}) \\ = m(\Delta\omega)\alpha e^{-i\Delta\omega\tau_{12}} - m(\Delta\omega)\frac{\alpha\beta^2}{4}(e^{-i\Delta\omega\tau_{12}} + e^{+i\Delta\omega\tau_{12}}). \end{aligned} \quad (35)$$

At times $t > \tau_{12}$ after the second pulse we then have

$$\begin{aligned} m_\perp(\Delta\omega, t) \\ = m(\Delta\omega)\alpha e^{-i\Delta\omega t} - m(\Delta\omega)\frac{\alpha\beta^2}{4}(e^{-i\Delta\omega t} + e^{-i\Delta\omega(t-2\tau_{12})}). \end{aligned} \quad (36)$$

The last term here gives the echo signal, whose maximum value is detected at the time $t = 2\tau_{12}$:

$$m_{\perp \text{ echo}}(t) = \frac{\alpha\beta^2}{4} m_0 \int g(\Delta\omega) e^{-i\Delta\omega(t-2\tau_{12})} d\Delta\omega. \quad (37)$$

We have ignored relaxation processes, which reduce the transverse component of each isochromatic curve and thereby reduce $m_{\perp \text{ echo}}(t)$. In many cases the damping is exponential. In such a case the total time dependence of the amplitude $m_{\perp \text{ echo}}(t)$ is given by

$$m_{\perp \text{ echo}}(t) = \frac{1}{4} m_0 \alpha \beta^2 e^{-t/\tau_{12}} \int g(\Delta\omega) e^{-i\Delta\omega(t-2\tau_{12})} d\Delta\omega. \quad (38)$$

The observable echo signal, i.e., the emf induced in the receiver, is

$$U_{\text{echo}} = c\omega_n \eta m_{\perp \text{ echo}}(t). \quad (39)$$

We have been discussing the two-pulse echo. Another important case is the three-pulse or so-called stimulated echo. The conventional mechanism for the formation of this echo can be outlined qualitatively as follows: After the first two pulses, the situation is precisely the same as in the case described above. Now, in contrast, we examine the changes in the longitudinal components which arise after the second pulse is applied (with $\beta < \pi$) due to the rotation of $m_y(\Delta\omega, \tau_{12})$ around the x axis. If the second pulse rotates the magnetization through an angle β , then each isochromatic grouping acquires an increment in the component $m_z(\Delta\omega)$; this increment depends on the phase of the grouping (Fig. 4b):

$$\Delta m_z(\Delta\omega, \tau_{12}) = -m(\Delta\omega) \alpha \beta \cos \Delta\omega \tau_{12}. \quad (40)$$

This correction to the longitudinal component is retained until the third pulse is applied. When this third pulse is applied, again along the x axis, at a time τ_{23} after the end of the second pulse, we find that $m_z(\Delta\omega)$ rotates through an angle ξ , and a new transverse component appears in the x, y plane:

$$m_{\perp}(\Delta\omega, t) = -m(\Delta\omega) \alpha \beta \xi e^{-i\Delta\omega(t-\tau_{23}-\tau_{12})} \cos \Delta\omega \tau_{12}. \quad (41)$$

As in (34), we have ignored a term which does not contribute to the echo. The subsequent rotation of the components $m_1(\Delta\omega, t)$ in the transverse plane causes these components to come into phase at the time $t = \tau_{23} + 2\tau_{12}$, and the amplitude of the resultant component is

$$m_{\perp \text{ echo}}(t) = \frac{1}{2} m_0 \alpha \beta \xi \int g(\Delta\omega) e^{-i\Delta\omega(t-\tau_{23}-\tau_{12})} d\Delta\omega. \quad (42)$$

Now considering relaxation processes, and assuming them to be exponential, we must multiply the right side of (42) by $\exp[-(\tau_{23}/T_1) - (2\tau_{12}/T_2)]$, where T_1 is the longitudinal relaxation time. We are thus taking into account that during the time interval between the first and second pulses and again between the third pulse and the echo signal relaxation occurs at the rate typical of the transverse components, while during the time interval between the second and third pulses relaxation occurs at the rate typical of the longitudinal component. If we furthermore take into account the spectral composition of the exciting pulses, i.e., if we no longer assume them to be δ -shaped pulses, we find that the expressions for the echo become more complicated. The corresponding analysis, which may be of interest primarily for applications, is set forth in Ref. 30, among other places.

Expressions (38) and (42) show that for an analysis of echo signals we must consider the frequency distribution of

the emission from the excited spin system. This distribution consists of the product of the complex function $m_{\perp}(\Delta\omega, t)$, which corresponds to the amplitudes and phases of the spin excitation, and the frequency distribution of these spins, $g(\Delta\omega)$. If the function $m_{\perp}(\Delta\omega, t)$ is of the form in (33), the echo signal does not form. The distortion of the function $m_{\perp}(\Delta\omega, t)$ due to the nonuniformity of the effect of the second rf pulse on the system of nuclear spins gives rise to the signals of the Hahn spin echo. In systems with a dynamic frequency shift, however, effects which give rise to a modulation of the function $g(\Delta\omega)$ are more important. This modulation gives rise to a new echo formation mechanism, the "frequency-modulation mechanism."

4. Frequency-modulated echo

The model of a frequency-modulation mechanism for the formation of an echo, originally proposed by Gould³¹ for a system of anharmonic oscillators, was first applied to nuclear spin systems with a dynamic frequency shift by Richards.³² This problem was solved more carefully in Ref. 33.

To simplify the analysis of the formation of the frequency-modulated echo as much as possible, we adopt the following assumptions for the time being:

1. The pulses applied to the nuclear system are applied without a frequency difference; i.e., their frequency is the NMR frequency.
2. The pulses are short enough that we may ignore the nonlinearity of the trajectories in the motion of the isochromatic groupings.
3. The angles through which the nuclear magnetization is deflected are small.
4. The deflection angles and the dynamic frequency shift ω_p are independent of $\Delta\omega$, i.e., are the same for all the isochromatic groupings.
5. Relaxation processes can be ignored.

In this case (i.e., with a dynamic frequency shift) it is important to consider not only the dynamics of the transverse components of the isochromatic grouping but also the changes in the m_z component of the nuclear magnetization, since the precession frequency of the isochromatic groupings depends on the value of m_z as shown in (1) and (15). After the first pulse, which rotates $m(\Delta\omega)$ through a small angle α , there is a decrease in the $m_z(\Delta\omega)$ components of all the isochromatic groupings by the same amount $\Delta m_z(\Delta\omega) = (1/2)m_0(\Delta\omega)\alpha^2$, so that there is a frequency shift $\Delta\omega''_{p\alpha} = (1/2)\omega_p\alpha^2$ in (15). Since this shift (under our assumptions) is the same for all the isochromatic groupings and is small in comparison with $1/\tau_1$, we need consider it no further. After the second pulse, as in the case of the Hahn model (Fig. 3c), the cone of nuclear isochromatic groupings is tilted at an angle β . There is again a decrease in all the $m_z(\Delta\omega)$ components by an amount $\Delta m_z(\Delta\omega) = (1/2)m_0(\Delta\omega)\beta^2$, and there is a corresponding common shift of the precession frequency of the isochromatic groupings by an amount $\Delta\omega''_{p\beta} = (1/2)\omega_p\beta^2$; for the time being, this frequency shift can also be ignored. In addition, however, there is a modulation of the $m_z(\Delta\omega)$ components of the isochromatic groupings described by

$$\Delta m_z(\Delta\omega) = -m_0\alpha\beta \cos \Delta\omega\tau_{12}, \quad (43)$$

caused by the rotation of the $m_y(\Delta\omega, \tau_{12})$ components. As a result, there is a nonuniform frequency shift of each isochromatic grouping by an amount⁶⁾

$$\Delta\omega_{p\beta}^\perp = \lambda \cos \Delta\omega\tau_{12}, \quad (44)$$

where

$$\lambda = \omega_p\alpha\beta.$$

The new frequency of the isochromatic grouping, which determines the change in its phase after the second pulse, is therefore

$$\Delta\omega' = \Delta\omega + \lambda \cos \Delta\omega\tau_{12}. \quad (45)$$

The resultant transverse magnetization at the time $t > \tau_{12}$ is described by

$$m_\perp(\Delta\omega, t) = m_0 \int g(\Delta\omega) [\alpha e^{-i[\Delta\omega\tau_{12} + \Delta\omega'(t-\tau_{12})]} + \beta e^{-i\Delta\omega'(t-\tau_{12})} + \Phi(\alpha\beta^2)] d\Delta\omega. \quad (46)$$

The first term here (proportional to α) describes the motion of the transverse components which arise after the first pulse, taking into account the change in their frequency, (45). The second term (proportional to β) describes the motion of the transverse components which arise after the second pulse, and the third term, $\Phi(\alpha, \beta^2)$, describes the changes in the isochromatic groupings which give rise to the ordinary echo. It is a simple matter to show that at small deflection angles $\alpha, \beta \ll \pi/2$ in the case of a large dynamic frequency shift ($\lambda\tau_{12} \gg \pi$) we can ignore this term.³³ The exponential functions can be written as an expansion in Bessel functions of the first kind:

$$e^{-i\lambda(t-\tau_{12})\cos\Delta\omega\tau_{12}} = \sum_{h=-\infty}^{\infty} (-i)^h J_h[\lambda(t-\tau_{12})] e^{ih\Delta\omega\tau_{12}}. \quad (47)$$

Making use of our assumptions regarding the uniformity of the deflection angles and of the dynamic frequency shift for all the isochromatic groupings, and also discarding all terms which are not pertinent here, we find the following expression for the resultant transverse magnetization which induces an echo through frequency modulation (the frequency-modulation mechanism):

$$m_\perp \text{ echo}(t) = m_0\alpha \sum_{h=2}^{\infty} (-i)^h J_h[\lambda(t-\tau_{12})] \int g(\Delta\omega) e^{-i\Delta\omega(t-h\tau_{12})} d\Delta\omega + m_0\beta \sum_{h=1}^{\infty} (-i)^h J_h[\lambda(t-\tau_{12})] \times \int g(\Delta\omega) e^{-i\Delta\omega[t-(h+1)\tau_{12}]} d\Delta\omega. \quad (48)$$

The amplitude of the echo signal which arises at the time $t = 2\tau_{12}$ is

⁶⁾By virtue of our assumptions (Section 1) we have ignored the effect of the change in the precession frequency, $\Delta\omega_{p\beta}^\perp$, on the motion of \mathbf{m} during the second rf pulse (since we have $\Delta\omega_{p\beta}^\perp \ll 1$ for linear trajectories), and we will take $\Delta\omega_{p\beta}^\perp$ into account only at $t > \tau_{12}$, since the condition $\tau_{12} \gg \tau_2$ usually holds.

$$U_{\text{echo}}(t) = c\tau\omega_n m_0 \sqrt{\alpha^2 J_2^2(\lambda\tau_{12}) + \beta^2 J_1^2(\lambda\tau_{12})}. \quad (49)$$

The formation of the frequency-modulated echo has some distinctive features. In contrast with the usual arrangement, the echo is formed not only by the transverse components which are excited by the first pulse (corresponding to the term proportional to α) but also, and directly, by the transverse components which are excited by the second pulse [corresponding to the term proportional to β in (46)]. In the ordinary Hahn echo the latter components cause only an induction. In the present case there is a sort of superposition of two signals which are $\pi/2$ out of phase.

A second distinctive feature is that the echo signals can arise not only at a time τ_{12} after the second pulse but also at subsequent times $k\tau_{12}$, as can be seen from (48).

Third, the time dependence of the echo intensity is governed not only by relaxation processes (which we are ignoring) but also by the t dependence of $J_k[\lambda(t-\tau_{12})]$.

The reader is referred to the original papers³³⁻³⁵ for more-general expressions incorporating the relaxation properties (and large rotation angles of the nuclear moments) and an expression for the stimulated-echo signal.

In concluding this subsection of the review we wish to emphasize that in analyzing the formation of the frequency-modulated echo we have worked from an expression for $m_\perp(\Delta\omega, t)$, (46), which corresponds to the linear approximation in the angles (α and β) describing the deflection of the nuclear magnetization; i.e., we have used an expression in a form analogous to (33). This analysis shows that, in contrast with the Hahn echo, which forms as a consequence of the nonuniformity of the interaction of the second pulse with the excited system of nuclear spins (Subsection II3), the mechanism for the formation of the frequency-modulated echo involves a corresponding change in the frequencies of the isochromatic groupings, (45), and in this case the Hahn contribution to the echo [the term $\Phi(\alpha\beta^2)$ in (46)] can be ignored. The change in the frequencies of the isochromatic groupings in (45) actually reduces to a change in the shape of the NMR line, $g(\Delta\omega)$, i.e., to a switch from $g(\Delta\omega)$ to $g(\Delta\omega')$. Although we cannot write an analytic expression for $g(\Delta\omega')$ in terms of the new variables, this function can be described numerically.³⁶ It turns out that the function $g(\Delta\omega')$ is a periodic function of $\Delta\omega'$ with a modulation period of $2\pi/\tau_{12}$ (Fig. 5). This

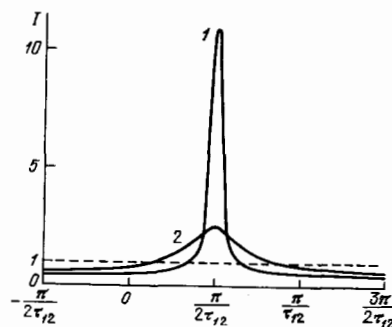


FIG. 5. Results of a numerical calculation [from Eq. (45)] of the change in the line shape in the frequency interval $-\pi/2\tau_{12} < \Delta\omega < 3\pi/2\tau_{12}$ under the influence of the second rf pulse, for two values of the parameter λ in (44) (Ref. 36): a— $1.22/\tau_{12}$; b— $0.61/\tau_{12}$. The unit along the intensity scale (the dashed line) is the unperturbed line intensity ($\lambda = 0$).

result essentially means that in adopting this renormalization we have obtained a set of oscillators which are grouped around characteristic frequencies separated by a frequency $2\pi/\tau_{12}$. The frequency mechanism for the echo modulation can then be described easily and clearly as corresponding to the beats from a set of oscillators whose frequencies differ by a common interval $2\pi/\tau_{12}$.

III. EXPERIMENTAL RESEARCH

5. Measurement methods

Most of the experiments have been carried out with standard spin-echo spectrometers.^{34,37,38} Figure 6 is a block diagram of the spectrometer. The control-pulse unit generates the appropriate sequence of video pulses of the appropriate length and controls the operation of the rf oscillator, which is tuned to the resonant frequency. The rf pulses are fed through attenuators, a circulator, and a matching device to the resonant system, which contains the test sample. The induction and echo signals which are formed in the sample by the rf pulses go from the resonant system through a matching device and a circulator to the receiver; then they are amplified and displayed on an oscilloscope screen. The oscilloscope is triggered by any of the video control pulses. In addition to these units, the spectrometer contains a power supply, units for measuring and regulating the temperature and the magnetic field, units for measuring the power of the rf pulses, and a circuit for monitoring the amplitude and shape of the rf pulses.

The spectrometers typically operate over a frequency range 100–3000 MHz, use rf pulses with a length $\tau \geq 0.5 \mu\text{s}$ and a power level $P \leq 10\text{--}30 \text{ W}$, and have a receiver with a sensitivity $\sim 10^{-13} \text{ W}$, a gain band of 1.0 MHz, and an interval of degraded sensitivity $\leq 4 \mu\text{s}$ long after the rf pulse.

The resonant system may be a spiral resonator,^{37,38} a short-circuited coaxial resonator with capacitance tuning,^{34,39} or a low- Q resonator consisting of a line of variable length and a short-circuited one- or two-turn coil.⁴⁰ Use of a spiral resonator can increase the amplitude of the rf field of the sample by 20–25 dB. A coaxial resonator and a resonator using a variable-length line are more convenient for tuning the frequency of the rf pulses.

All published experiments on the nuclear echo in systems with a dynamic frequency shift have been carried out at low temperatures (4.2 K and below), since it is only under these conditions that the dynamic frequency shift is large enough.

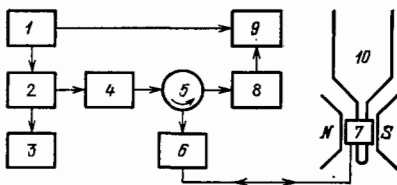


FIG. 6. Block diagram of the spectrometer. 1—Unit which generates a programmed sequence of video pulses; 2—rf oscillator; 3—wave meter; 4—attenuator; 5—circulator; 6—matching device; 7—resonant system; 8—receiver; 9—oscilloscope; 10—glass cryostat.

6. Magnetically ordered crystals which have been studied

The nuclear echo in a system with a dynamic frequency shift was initially observed³² in the antiferromagnetic substance MnO , which has an orthorhombically distorted cubic magnetic structure. In contrast, most of the experimental results on the properties and dynamics of nonlinear nuclear spin systems with a dynamic frequency shift have been obtained in studies of the spin systems of Mn^{55} nuclei in single crystals of the antiferromagnetic materials MnCO_3 , CsMnF_3 , and RbMnF_3 (Refs. 41 and 42). These crystals are convenient in that the dynamic frequency shift in them is large enough to work with even at liquid-helium temperature (Table I). Furthermore, these antiferromagnetic materials have a rather simple structure and have been studied extensively.

Manganese carbonate (MnCO_3) is a two-sublattice antiferromagnetic material with an easy-plane anisotropy and a weak ferromagnetic moment in its basis plane. No anisotropy has been observed in the basis plane. The NMR frequency and the dynamic frequency shift are described satisfactorily by expressions (1) and (18) (Fig. 7).

Antiferromagnetic CsMnF_3 is also an easy-plane antiferromagnetic substance. This crystal has the distinguishing property that the Mn^{2+} ions occupy two crystallographically nonequivalent positions. The electron spins form ferromagnetic planes perpendicular to the c hexagonal axis. Each ferromagnetic plane contains Mn^{2+} ions of only a single type; adjacent ferromagnetic planes are oriented in an antiferromagnetic fashion. Because of the crystallographic nonequivalence of the Mn^{2+} ions, the hyperfine fields for them are slightly different. The spectrum of bound electron-nuclear oscillations thus contains two characteristic frequencies: $\omega'_{n0}/2\pi = 666 \text{ MHz}$ and $\omega''_{n0}/2\pi = 676.85 \text{ MHz}$. Correspondingly, we find two "shifted" NMR branches ω'_n and ω''_n , one of which corresponds to an in-phase motion of the magnetizations of the nuclei in both positions. Under the condition $\omega_p \gg |\omega'_{n0} - \omega''_{n0}|$, this branch is described well by Eq. (16). The frequencies of the other branch correspond to an out-of-phase motion of the nuclear magnetization and lie between ω'_{n0} and ω''_{n0} .

Below the magnetic ordering point ($T_N = 82.6 \text{ K}$) the RbMnF_3 crystal is an ideal, cubic, strictly collinear antiferromagnetic material with an ordering direction along the [111] threefold axis. An external magnetic field deflects the sublattice magnetizations away from easy axes, and at $H_0 > H_c = 2.3 \text{ kOe}$ the magnetizations of the sublattices lie in a plane perpendicular to the external magnetic field. An angle $\xi = H_0/H_E \ll 1$ arises between the magnetizations in the direction of the external field H_0 . From the magnetic standpoint, cubic RbMnF_3 at $H_0 > H_c$ is essentially identical to an easy-plane antiferromagnetic material.⁹

In addition to these crystals, there are several others in which a dynamic frequency shift has been observed directly; the ferrite MnFe_2O_4 and antiferromagnetic FeBO_3 are particularly noteworthy. The dynamic frequency shift for nuclei in the domains in a ferrite is very small, since its structure is not as sensitive to the anisotropy fields as in an antiferromagnetic substance. Direct observation of the dy-

TABLE I. Characteristics of the spin systems exhibiting a dynamic frequency shift. AFM—Antiferromagnetic substance; WF—weak ferromagnetism; FM—ferrite; PE—parametric echo; FME—frequency-modulated echo; CN—continuous NMR method; I—induction signal; H—Hahn-echo method.

Material	Nu- cleus	ν_{n0}	ν_e	ν_Δ	$\nu_{p \max}$	Method
CsMnF ₃ , AFM	Mn ⁵⁵	666 MHz 677 MHz	$\gamma_e^2 H^2 + \nu_\Delta^2$, $\gamma_e = 2.8 \cdot 10^6$ Hz/Oe	$7.08/\sqrt{T}$ (AFM) $6.8/\sqrt{T}$ (NMR)	506 MHz (2K) 166 MHz (4.2–0.04 K)	PE FME
MnCO ₃ , AFM WF	Mn ⁵⁵	640 MHz	$\gamma_e^2 H (H + H_D) + \nu_\Delta^2$, $\gamma_e = 2.8 \cdot 10^6$ Hz/Oe, $H_D = 4.4$ kOe	$6.7/\sqrt{T}$ GHz	140 MHz (4.2–0.04 K)	PE, FME
RbMnF ₃ , AFM	Mn ⁵⁵	686 MHz	$\gamma_e^2 (H^2 - H_c^2) + \nu_\Delta^2$ ($H \parallel [100]$), $H_c = 2.25$ kOe	$11/\sqrt{T}$ GHz	406 MHz 78 MHz 186 MHz	CN FME PE
RbMnCl ₃ AFM	Mn ⁵⁵	600* MHz 627* MHz	$\gamma_e^2 (H^2 - H_c^2 \cos 2\varphi) + \nu_\Delta^2$, $\gamma_e = 2.8 \cdot 10^6$ Hz/Oe, $H_c = 6.6$ kOe	$10.7/\sqrt{T}$ GHz (AFMR) $14.5/\sqrt{T}$ * GHz (NMR, $H > H_c$) $9.7/\sqrt{T}$ * GHz (NMR, $H < H_c$)	100* MHz (4, 2 K)	PE
MnO, AFM	Mn ⁵⁵	624 MHz	$\gamma_e^2 H^2 \cos^2 \psi + \nu_\Delta^2$, $\gamma_e = 2.8 \cdot 10^6$ Hz/Oe	The AFMR and NMR data do not agree	25 MHz (4.2 K)	FME
KMnF ₃ , AFM	Mn ⁵⁵	676 MHz	Complex spectrum	$\sim 11/\sqrt{T}$ GHz	97 MHz	CN
MnF ₂ , AFM	Mn ⁵⁵	760 MHz ($H = 90$ kOe)	$\gamma_e^2 (H_c - H)^2 + \nu_\Delta^2$, $H_c = 92.92$ kOe, $\gamma_e = 2.8 \cdot 10^6$ Hz/Oe	$\sim 0.8/\sqrt{T}$ GHz	15 MHz (1.5 K, 92 kOe)	CN
FeBO ₃ , AFM, WF	Fe ⁵⁷	76,442 MHz	$\gamma_e^2 H (H + H_D) + 38^2$ GHz, $H_D \approx 100$ kOe, $\gamma_e = 2.8 \cdot 10^6$ Hz/Oe ($T = 4.2$ K)	$90/\sqrt{T}$ MHz	2 kHz (2 K)	I
CoCO ₃ , AFM, WF	Co ⁵⁹	220* MHz	$\gamma_e H (H + H_D) + \nu_\Delta^2$, $\gamma_e = 4.4 \cdot 10^6$ Hz/Oe, $H_D = 51.5$ kOe	$2.2/\sqrt{T}$ GHz Calculated	Not observed	H
MnFe ₂ O ₄ , FM	Mn ⁵⁵	578 MHz	~ 8.4 GHz + ν_Δ ($H = 0$)	$\frac{570}{T}$ kHz ($T > 0.1$ K)	10 MHz (0,04 K)	I
He ³	He ³	$\gamma_n H$ $= 324$ kHz/Oe	Superfluid: α -phase	$\nu^2 = (\gamma H)^2 + \nu_L^2 \left(\frac{1+3 \cos \varphi}{4} \right)$	$\nu_{L \max}$ 150 kHz ($2 \cdot 10^{-3}$ K)	I
			β phase	More complicated spectrum	300 kHz ($0.8 \cdot 10^{-3}$ K)	I
Solid: frequency-modulated echo observed at $T = 0.02$ K						

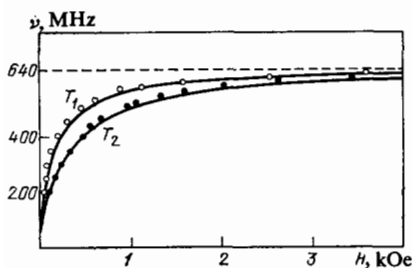


FIG. 7. The NMR frequency of Mn⁵⁵ in MnCO₃ as a function of the external magnetic field H at the temperatures $T_1 = 4.2$ K and $T_2 = 1.8$ K (Ref. 9). The unshifted NMR frequency is $\nu_0 = 640$ MHz.

dynamic frequency shift thus requires working at temperatures in the interval 40–100 mK, which have been attained in a cryostat⁴³ based on dissolution of H³ in He⁴. The dynamic shift of the NMR frequency of Mn⁵⁵ nuclei at domain walls in MnFe₂O₄ has been found to be much larger in magnitude (and opposite in sign).⁴⁴ In this case the shift can be observed even at $T = 1.7$ K (see Subsection 11). A dynamic frequency shift has also been observed at $T = 1.7$ K for Eu¹⁵¹ nuclei at domain walls in the ferrite⁴⁵ Eu₃Fe₅O₁₂.

Antiferromagnetic FeBO₃ is the first medium in which a dynamic frequency shift has been observed for Fe⁵⁷ nuclei.

Because of the low natural abundance of these nuclei ($\sim 2\%$) and their small magnetic moment, and also because of the large magnetoacoustic gap in the antiferromagnetic resonance spectrum of FeBO_3 , the dynamic frequency shift is very small and has been observed directly at liquid-helium temperature by means of the phase-detection regime on a Bruker SXP-4-100 spectrometer⁴⁶ (Subsection 9). We might also mention a report⁴⁷ of a dynamic frequency shift for Co^{59} nuclei in thin ferromagnetic films containing cobalt.

Table I lists characteristics of the crystals in which a dynamic frequency shift has been observed. The fourth column gives the spectra of the low-frequency antiferromagnetic resonance (or ferromagnetic resonance); the fifth gives the shift of the AFMR frequency caused by the hyperfine field of the nuclei. From these results we can easily find ω_n using $\omega_{n0}\omega_e = \omega_n \sqrt{\omega_e^2 + \omega_d^2}$. The sixth column shows the maximum dynamic frequency shifts which have been observed by the various methods, which are themselves listed in the seventh column.

Shown at the end of the table are data on nonlinear aspects of the nuclear magnetic resonance in the superfluid and solid phases of He^3 , which also exhibit effects analogous to a dynamic frequency shift. This table was compiled from the data of Refs. 22, 37, and 48 on CsMnF_3 ; Refs. 21, 37, 49, and 50 on MnCO_3 ; Refs. 51, 42, and 52 on RbMnF_3 ; Ref. 53 on RbMnCl_3 ; Refs. 32 and 54 on MnO ; Ref. 20 on KMnF_3 ; Ref. 55 on MnF_2 ; Refs. 46, 10, and 56 on FeBO_3 ; Ref. 43 on MnFe_3O_4 ; and Refs. 57-59 on He^3 . The asterisk marks some previously unpublished results found by Bun'kov and Maksimchuk.

7. Free-induction signal

The simplest way to study the dynamics of the motion of nuclear spins experimentally is to study the free-induction signal after a sufficiently short rf pulse ($\tau \ll T_2^*$). In this case, if the angle through which the nuclear magnetization is deflected is small, the signal amplitude is proportional to the spin rotation angle at the end of the rf pulse, (30). In the case of systems with a dynamic frequency shift, however, this method is not very informative, because of several experimental difficulties: the difficulty in arranging the condition $\tau \ll T_2^*$, the relatively long time intervals during which the receiver is insensitive after the rf pulse, and the choppiness of the induction signal,^{32,37} which makes it impossible to extrapolate the intensity of the induction signal to the end of the rf pulse.

It has nevertheless been found possible to carry out several qualitative studies of the induction signal in MnCO_3 . In particular, measurements of the frequency of the induction signal through fine tuning of a superheterodyne receiver have made it possible to observe directly a frequency shift of the spin precession as a function of the power level of a short rf pulse³⁷ (Fig. 8). It turns out that the maximum change in the frequency is of the order of the reciprocal of the pulse length and is accompanied by a significant broadening of the NMR line. Furthermore, the curves of the intensity of the induction signal as a function of the length and power of the rf pulses shown in Ref. 37 demonstrate that the intensity of

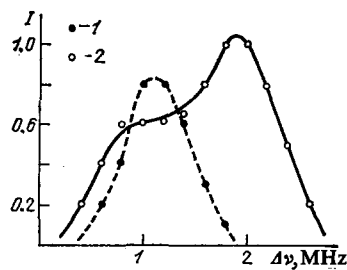


FIG. 8. Intensity of the free-precession signal as a function of the frequency to which the superheterodyne receiver is tuned.³⁷ 1—Low power level of the rf pulses; 2—near the maximum signal amplitude ($\Delta\nu$ is the difference between the frequency to which the receiver is tuned and a reference frequency).

the induction signal goes through a maximum. Figure 9 shows the length of the rf pulse at which the signal reaches its maximum as a function of the pulse power P . We see that this function is described satisfactorily by the expression $\tau^{-3} \sim P$. These results can be explained by assuming that the angle through which the spins rotate is restricted by the frequency difference which arises between the rf pulse and the NMR frequency of the excited spin system. It follows from the theory for the dynamics of the motion of a spin system with a dynamic frequency shift (Ref. 27) that the first maximum in the dependence of the precession amplitude on the pulse power is reached under the condition

$$\tau^{-3} \sim (\eta^2 \omega_p) \gamma^2 h_1^2. \quad (50)$$

Expression (50) not only agrees with the experimental dependence (taking into account that $P \sim h_1^2$) but also explains the different slopes of the lines for various observation temperatures (Fig. 9). As the temperature is lowered, at a constant NMR frequency, the external magnetic field required for observation of the NMR increases. The result is a decrease in the gain η and thus a decrease in the slope of the $\tau^{-3} \sim P$ dependence.

8. Spin-echo signals

Experimental research on the mechanism of formation of the spin echo in systems with a dynamic frequency shift has moved well ahead of the corresponding theoretical work and has stimulated the latter. This is true of the first observation of spin-echo signals, whose existence had been the sub-

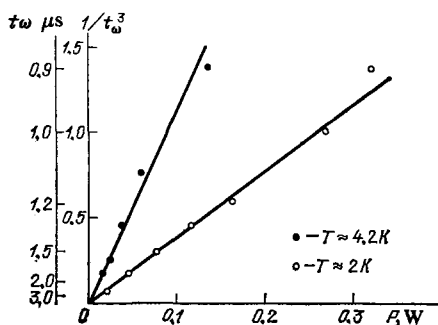


FIG. 9. The length (t_w) of the rf pulses at which the free-induction signal reaches its maximum as a function of the power level of the pulses ($\nu_{\text{NMR}} = 610 \text{ MHz}$).³⁷

ject of some theoretical debate, and also true of essentially all the other effects which have been found. For simplicity, however, we have grouped most of the theoretical ideas regarding the mechanisms of echo formation in the early part of this review. In this experimental part we are thus discussing specific experimental effects, and we will pay particular attention to how well they are described theoretically.

Echo signals in systems with a dynamic frequency shift were first observed nearly simultaneously by three research groups in MnO (Ref. 32), CsMnF₃ and MnCO₃ (Ref. 41), and RbMnF₃ (Ref. 42) at liquid-helium temperature. The first experiments revealed several unusual properties of the echo signals in these systems: a large echo amplitude when the angles through which the spins are deflected by the rf pulses are small,^{33,37} the existence of secondary echo signals at the times $k\tau_{12}$ (Refs. 33, 41, and 42), a temporal shift of the position of the echo signal away from $2\tau_{12}$ (Ref. 60), and an intensification of the echo signal when a preliminary pulse is applied.³² It was found that these properties of the echo cannot be described by the conventional Hahn model⁴ (Section 3). These effects do agree, on the other hand, with the theory which has been derived for the frequency-modulated echo. Let us examine the most important aspects of the frequency-modulated echo.

Figure 10 shows the echo intensity as a function of the power level of two identical rf pulses in cases of resonant and nonresonant excitation according to Ref. 37. The solid curve is the theoretical function (49). The intensities, both theoretical and experimental, are plotted in arbitrary units. According to estimates the position of the intensity maximum agrees in order of magnitude with the theoretical position, and this maximum occurs when the nuclear spins are deflected through an angle $\sim 1^\circ$. At large amplitudes of the rf excitation of the spins we see a sharp decrease in the intensity of the echo signal associated with an increase in the relaxation rate.

According to the theory, the intensity of the frequency-modulated echo is the sum of the two terms $\alpha J_2(\lambda\tau_{12})$ and $\beta J_1(\lambda\tau_{12})$ [see (49)]; by varying the parameters of the pulses one can bring out directly either the α or the β mechanism for the echo formation.⁷⁾ At small deflection angles the in-

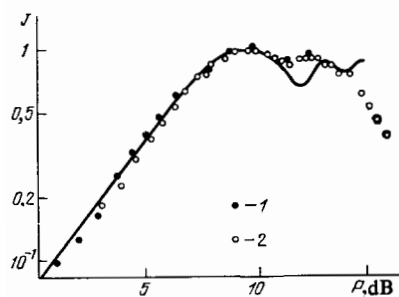


FIG. 10. Intensities of the spin-echo signals as functions of the power level of the rf pulses.³⁷ 1—Two-pulse echo; 2—single-pulse echo. The solid curve is theoretical.

⁷⁾The concept of α and β mechanisms for the formation of the frequency-modulated echo, reflecting the physical nature of the two terms in Eq. (49) (Section 4), was originally introduced by Petrov *et al.*³³ The contributions of each of the mechanisms to the frequency-modulated echo have been distinguished experimentally by a phonon-pumping mechanism.⁶¹

tensity of the α echo is proportional to $\alpha^2\beta$, while that of the β echo is proportional to $\alpha\beta^2$. Experiments carried out with separate changes in the intensities of the rf pulses, however, yielded results at odds with the theory. The rf pulses made roughly equal contributions to the intensity of the echo signal ($\alpha^{1.5}\beta^{1.5}$) over broad ranges of α and β .

On the other hand, the Bessel functions $J_{1,2}(\lambda\tau_{12})$ in the expression for the frequency-modulated echo, (49), can be of the order of unity even under the conditions $\alpha, \beta \ll 1$, but with ω_p sufficiently large. The intensity of the frequency-modulated echo can thus be proportional to the first power of the angle through which the nuclear magnetization is deflected (α or β). Since these angles were $\alpha, \beta \sim 10^{-2}$ rad under conditions with a dynamic frequency shift, (1), in the experiments of Refs. 32, 41, and 42, the intensity of the frequency-modulated echo can be $\sim 10^4$ times that of the ordinary Hahn echo with identical amplitudes of the exciting pulses.

An important distinguishing feature of the frequency-modulated echo is that it can be excited in a "nonresonant" fashion, by which we mean that the nuclear-echo signal can be observed when the frequency of the rf pulses differs from the NMR frequencies of the spins by an amount greater than the width of the NMR line ($|\Delta\omega| = |\omega_n - \omega| > 2\pi/T_2^*$). Furthermore, the condition $\omega_1 \ll |\Delta\omega|$ must hold, where $\omega_1 = \gamma\eta h_1$ is the amplitude of the rf pulses expressed in frequency units. The Hahn mechanism is naturally ineffective in nonresonant excitation because of the small deflection angles.⁶² The frequency-modulated echo, in contrast, is observed when there is a substantial difference between the frequencies of the rf pulses and the NMR frequency (Fig. 11). Furthermore, the maximum intensities of the frequency-modulated echo in the case of nonresonant excitation and in the case without a frequency difference (resonant excitation) are comparable.^{37,63} In the case of nonresonant excitation the frequency-modulated echo reaches its maximum at a power level of the rf pulses proportional to the square of the frequency difference being used. This result means that the echo reaches its maximum intensity at the same spin-deflection angle. It should be noted that in the case of nonresonant excitation the frequency of the frequency-modulated echo is equal to the NMR frequency given by (15)–(18).

The reason why nonresonant excitation of the frequency-modulated echo is possible is that the frequency-modulation mechanism for the production of the two-pulse echo is

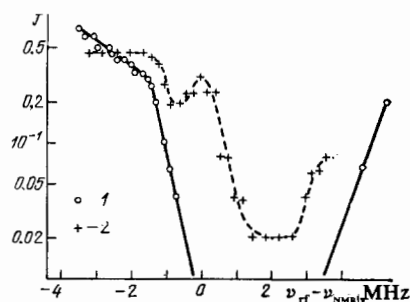


FIG. 11. Maximum intensities of the single-pulse (1) and two-pulse (2) echos as functions of the difference between the frequency of the exciting pulses, ν_{rf} , and the NMR frequency ν_{NMR} (Ref. 37).

effective only when the change in the dynamic frequency shift during the rf pulses can be ignored. This situation corresponds to a motion of the nuclear magnetization vector along linear trajectories or linear parts of trajectories during the rf pulse (see Section 2).⁶⁴ As we have already mentioned, this case arises either without a difference between the NMR frequency and the frequency of the rf pulses (in the case of short pulses) or in nonresonant excitation. The presence in the dependence of the echo intensity on the frequency difference of two regions in which there is an optimum formation of the two-pulse frequency-modulated echo (Fig. 11) demonstrates the validity of the theoretical conclusions. As we have already mentioned, small spin-deflection angles in the case of nonresonant excitation are acceptable for the frequency-modulation mechanism for the formation of an echo. Furthermore, the broad minimum in the echo intensity at $\omega_{\text{rf}} > \omega_n$ implies that the echo signal is formed only poorly in the region corresponding to trajectories with the greatest nonlinearity (near an aperiodic trajectory). These experiments thus furnish qualitative confirmation of the theory for the motion of spins in systems with a dynamic frequency shift.

Studies of the properties of the two-pulse frequency-modulated echo under conditions of nonresonant excitation have shown that, as in the case of resonant excitation, the amplitude of the echo signal reaches a maximum when the rf pulses are of equal length.⁶⁵ With increasing frequency difference, the echo amplitude increases with a decrease in the pulse length. This experimental result agrees with the theory for the formation of a frequency-modulated echo under nonresonant-excitation conditions³⁶; this theory shows that the first maximum on the curve of the echo amplitude as a function of the frequency difference is reached at pulse lengths

$$\tau_1 = \tau_2 = \frac{\pi}{\Delta\omega_0}. \quad (51)$$

Experiments also reveal oscillations in the echo amplitude as a function of the frequency difference with a period $\Delta\omega = 2\pi/\tau$; these oscillations are characteristic of a nonresonant excitation of echo signals.^{65,36}

These results pointed out the need for a detailed examination of the various possibilities for the formation of echo signals when spin systems are excited by pulses of a nonresonant rf field. These studies led to the revelation of an intense single-pulse echo⁸⁾ (Fig. 12),^{37,66} which is observed when a spin system with a dynamic frequency shift is excited by a sufficiently long rf pulse ($\tau \sim 30\text{--}100 \mu\text{s}$).

The single-pulse echo arises at times which are multiples of the pulse length, and its frequency and width are determined by the intrinsic resonant characteristics of the spin system. In principle, the single-pulse echo could also be observed in spin systems lacking a dynamic frequency shift (either nuclear or electron systems),^{68,67} but in a nuclear spin system with a dynamic frequency shift this effect would have

⁸⁾Studies of the single-pulse echo in crystals with a dynamic frequency shift stimulated a more detailed study of this effect in ordinary spin systems. The physical nature of single-pulse effects in spin systems has now been established. It turns out that the method of the single-pulse echo can reveal essentially the same information as that revealed by the method of the Hahn two- and three-pulse echos.^{68,70}

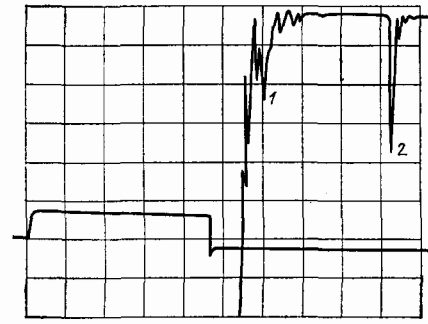


FIG. 12. Oscilloscope trace of the single-pulse echo of Mn^{55} in MnCO_3 (Ref. 66). 1—Free-induction signal; 2—single-pulse echo; lower trace—signal from the wave meter, demonstrating the length and position of the rf pulse (the pulse is $47 \mu\text{s}$ long).

some important features which would distinguish it from the effect in ordinary media. In MnCO_3 , for example, experiments have revealed not only a primary single-pulse echo at $t = \tau$ but also secondary signals at 2τ and 3τ . The single-pulse echo is observed only during nonresonant excitation (Fig. 11). The minimum frequency difference at which the signal can be observed is 0.5 MHz (the corresponding width of the NMR line in MnCO_3 is 0.3 MHz). We should also note the high intensity of the single-pulse echo, which is close to that of the two-pulse echo. In nuclear spin systems lacking a dynamic frequency shift the maximum intensity of the single-pulse echo does not exceed 10–15% of the maximum intensity of the two-pulse echo.⁶⁸ Finally, in MnCO_3 the amplitude of the single-pulse echo is highly dependent on the rise time of the rf exciting pulse. As this rise time is increased from 0.3 to $0.8 \mu\text{s}$ the echo amplitude falls off by an order of magnitude.

The formation of a single-pulse echo can be outlined as follows: During the pulse of the nonresonant rf field, the duration (τ) of the motion of an individual isochromatic grouping in the rotating coordinate system is a precession around the effective field \mathbf{H}_{eff} (Fig. 2b). In the approximation linear in θ the expression for $m_{\perp}(\Delta\omega, t)$ at $t > \tau$ can then be written by analogy with (33):

$$m_{\perp}(\Delta\omega, t) = i[\theta m(\Delta\omega) e^{-i\Delta\omega t} - \theta m(\Delta\omega) e^{-i\Delta\omega(t-\tau)}]. \quad (52)$$

Expression (52) describes the induction signals after the rise of the rf pulse. We first consider a spin system without a dynamic frequency shift.

To obtain a single-pulse echo we must take into account the ellipsoidal nature of the precession of the isochromatic-grouping vectors in the xy plane during the pulse (Fig. 2b). In this case we may ignore the second term in (52) [as in (33)]. The expression for $m_{\perp}(\Delta\omega, t)$ at the end of the pulse, $t = \tau$,

$$\begin{aligned} m_x(\Delta\omega, \tau) &= -\theta m(\Delta\omega) \left(1 - \frac{\theta^2}{2}\right) \cos \Delta\omega' \tau, \\ m_y(\Delta\omega, \tau) &= \theta m(\Delta\omega) \sin \Delta\omega' \tau, \end{aligned} \quad (53)$$

is then essentially the same as (34) with $\Delta\omega' = \sqrt{\Delta\omega^2 + \omega_1^2}$. Carrying out the calculations by the standard approach, which is described in the analysis of the two-pulse Hahn echo, (35)–(37), we then find the term which determines the single-pulse echo:

$$m_{\perp \text{echo}}(t) = im_0 \frac{\theta^3}{4} e^{-(t+\tau)/T_2} \int g(\Delta\omega) e^{-i(\Delta\omega t - \Delta\omega'\tau)} d\Delta\omega. \quad (54)$$

The time t is reckoned from the end of the pulse in this case. A distinguishing feature of the single-pulse echo is that the phase $\Delta\omega t - \Delta\omega'\tau$ in (54) does not vanish completely at any value of t , so that single-pulse echo signals can arise only under certain conditions, when this requirement is met sufficiently well. Analysis⁶⁸ shows that with nonresonant excitation the time corresponding to the maximum intensity of the single-pulse echo is

$$t = \tau \frac{\Delta\omega_0}{\sqrt{\Delta\omega_0^2 + \omega_0^2}}, \quad (55)$$

where $\Delta\omega_0$ is the difference between the frequency of the rf pulse and the center of the excited part of the NMR line. The phase of the echo is essentially the same as that of the rf pulse, (54).

The single-pulse echo in spin systems with a dynamic frequency shift is distinguished by the circumstance that, as in the case of the two-pulse frequency-modulated echo (Section 4), the mechanism for the formation of the single-pulse echo involves a corresponding change in the frequencies of the isochromatic groupings.^{29,66,69} At the end of the exciting pulse, the z component of the nuclear magnetization of the isochromatic grouping [which determines the frequency of the precession of this grouping after the pulse, according to (15)] depends on the phase of the isochromatic grouping (Fig. 2b). Calculations of the amplitude of the single-pulse frequency-modulated echo are quite complicated because the effect of the dynamic frequency shift on the motion of the isochromatic groupings during the pulse must be taken into account in this case.^{29,69} Under certain simplifying assumptions,⁶⁹ however, the expression for the amplitude of the single-pulse frequency-modulated echo is essentially the same as that for the two-pulse frequency-modulated echo. (49), if we set $\alpha = \beta = \theta$ in (49). Calculations show that the "Hahn" contribution, (52)–(55), to the amplitude of the single-pulse echo can be ignored in a spin system with a large dynamic frequency shift (as in the case of the two-pulse echo).

We now see why the amplitudes of the single- and two-pulse frequency-modulated echos depend on the experimental conditions in essentially the same way during nonresonant excitation (see Fig. 10, for example). The need to take into account the effect of the dynamic frequency shift on the motion of the isochromatic groupings during the pulse in the case of the single-pulse frequency-modulated echo, however, leads to more-stringent requirements on the linearity of the trajectories of the isochromatic groupings. This situation is seen experimentally in the circumstance that the single-pulse frequency-modulated echo is a definitely nonresonant effect (Fig. 11).

Let us consider yet another interesting property of the spin echo in a system with a dynamic frequency shift: the formation of secondary echo signals at the times $k\tau_{12}$ ($k = 3, 4, \dots$).^{3,41,42} Up to seven such signals have been detected experimentally. We should point out that, in general, secondary signals could also arise in systems lacking a strong dynamic frequency shift, as a consequence of quadrupole split-

ting⁷¹ or a self-effect mechanism,⁷² for example. In the latter case the self-effect might be that the emf induced in the resonator (or circuit) when the resultant spin moment comes into phase essentially plays the role of an auxiliary rf field acting on the spin system. The in-phase resultant nuclear moment itself leads to an analogous effect; it works through the hyperfine interaction to give rise to a resultant alternating field at the nuclei and thus a rotation of the nuclear magnetization. In this case, no external electric circuit need be involved.

In contrast with the Hahn echo, however, the secondary echo signals in spin systems with a dynamic frequency shift are an inseparable property of the frequency-modulation mechanism for the echo formation, (48). The nature of this effect can be described quite clearly. We have already seen that the formation of the frequency-modulated echo can be easily represented as the beats from a set of oscillators which differ in frequency by the same interval $2\pi/\tau_{12}$ (Section 4). These "beats," observed as echo signals, will of course be detected at the times $t = k\tau_{12}$.

A clear distinguishing feature of the frequency-modulated echo is a strong dependence of the time at which the echo appears on the experimental conditions. By "time of appearance" here we mean the time corresponding to the observation of the maximum echo intensity. We recall that the shift of the time at which the Hahn echo appears from the value $t = 2\tau_{12}$ can occur only within a range not exceeding the length of the exciting pulses.⁷³ On the other hand, it has been established experimentally that the time at which the frequency-modulated echo appears is determined by the frequencies of the rf pulses used, by the length of these pulses (Fig. 13), and, in particular, by the frequency difference between the NMR frequency and the frequency of the exciting rf pulses (Fig. 14).^{39,63,65} As the power level of the rf pulses is increased, the range of the time (t') at which the frequency-modulated echo appears becomes larger. The maximum deviations of t' from $2\tau_{12}$ reach 40% of τ_{12} . At high power levels of the rf pulses, the change in the time at which the frequency-modulated echo appears is an odd function of the frequency difference; i.e., $t' - 2(\tau_{12} + \tau) = f(\Delta\omega_0)$, where $f(\Delta\omega_0)$ is an odd function of $\Delta\omega_0$ (Fig. 14).

The particular nature of the temporal shift of the frequency-modulated echo is a consequence of the inhomoge-

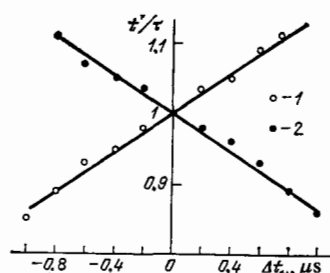


FIG. 13. Relative shift in the time in which the echo appears, T'/τ , as a function of the difference between the lengths of the exciting rf pulses,⁶⁰ $\Delta t_w = \tau_1 - \tau_2$. 1— $\tau_1 = 2\mu\text{s}$; 2— $\tau_2 = 2\mu\text{s}$. The time interval between the rf pulses is $50\mu\text{s}$; $\nu_{\text{NMR}} = 625\text{ MHz}$; $T = 1.8\text{ K}$.

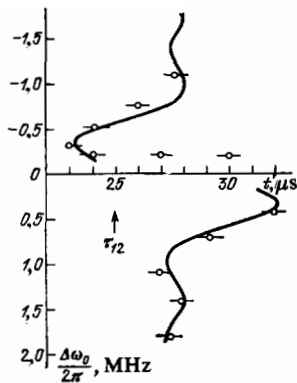


FIG. 14. Time at which the echo appears, T' , as a function of the difference between the carrier frequency of the rf pulses and the frequencies to which the receiver is tuned. Experiments for Mn^{55} in RbMnF_3 with $T = 1.7$ K, $\tau_{12} = 25 \mu\text{s}$, $\omega_p/2\pi = 45$ MHz, and $\nu_{\text{NMR}} = 633$ MHz. The solid curve is calculated from Eq. (22) in Ref. 36.

neity of the change in the spin precession frequency during the application of the second rf pulse, which changes the average distance, in frequency units ($\Delta\omega = 2\pi/\tau_{12}$), between those maxima of the spectral density which are formed from the generally monotonic NMR line shape by the second rf pulse. For the case of nonresonant excitation and under the condition $\tau_{12} > T_2$, which holds in RbMnF_3 , it has been found possible to find explicitly how the time (t') at which the frequency-modulated echo appears depends on the observation conditions (Fig. 14). These results explain the odd dependence of t' on the frequency difference.³⁶ This effect can be explained qualitatively by saying that with nonresonant excitation, in the case $|\Delta\omega| < 2\pi/\tau$, those spins which have a resonant frequency relatively close to the frequency of the rf pulses are deflected through greater angles, and their frequencies shift by a greater amount, in accordance with (15). As a result, for $\omega > \omega_n$ ($\Delta\omega < 0$) the distance between the maxima of the function $g(\Delta\omega')$ becomes greater than $2\pi/\tau_{12}$, and the frequency-modulated echo is formed before the time $2\tau_{12}$. In the opposite case, $\omega < \omega_n$ ($\Delta\omega > 0$), the distance between the maxima of the function $g(\Delta\omega')$ becomes smaller than $2\pi/\tau_{12}$, and the frequency-modulated echo is formed after the time $2\tau_{12}$. Under the condition $|\Delta\omega| > 2\pi/\tau$, the shifts of the various maxima of the function $g(\Delta\omega')$ may be irregular. In this case, the shift in the time at which the frequency-modulated echo appears may be accompanied by a splitting of this echo and by a substantial decrease in the intensity.³⁶

An experiment has been carried out to observe directly, the modulation of the spectral density of the NMR line, $g(\Delta\omega')$, under the influence of a second rf pulse; i.e., an experiment was carried out to detect "oscillators" with a frequency interval $2\pi/\tau_{12}$ (Fig. 5). In RbMnF_3 , because of the short transverse relaxation time T_2 , the spin echo is determined primarily by the second term in (49). Expression (49) for the amplitude of the frequency-modulated echo which appears at the time $t = 2\tau_{12}$ can be rewritten as follows, where we are taking into account relaxation processes and the unperturbed shape of the $g(\Delta\omega)$ line:

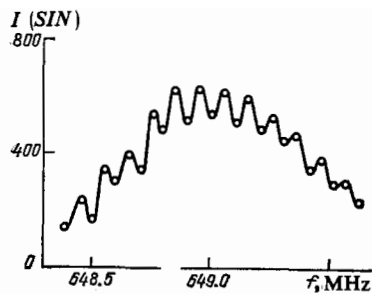


FIG. 15. Oscillation in the intensity of the Mn^{55} echo in RbMnF_3 as the receiver frequency is tuned. $\tau_{12} = 10 \mu\text{s}$, $T = 1.6$ K. The passband of the receiver is 1 MHz.

$$U_{\text{echo}}(t) = c\eta m_0 \omega_n e^{-\tau_{12}/T_2} \times \int \sqrt{\alpha^2 J_2^2(s) e^{-2\tau_{12}/T_2} + \beta^2 J_1^2(s)} g(\Delta\omega) d\Delta\omega, \quad (56)$$

where $s = \omega_p \alpha \beta \tau_{12} e^{-\tau_{12}/T_2}$. In this situation the spectrum of the observed frequency-modulated echo essentially corresponds to the spectral density $g(\Delta\omega')$, in which we are interested; i.e., the formation of an echo by the β mechanism is reflected most accurately by this qualitative model (beats of oscillators).

In the corresponding experiments, the NMR line in RbMnF_3 was excited by two rf pulses and scanned by a receiver with a square selectivity characteristic. The receiver recorded a periodic change in the number of maxima found in the function $g(\Delta\omega')$ (Fig. 5), as was seen in oscillations of the echo intensity (Fig. 15). A similar effect was observed for the free-induction signal after the second rf pulse and also for the secondary and stimulated echo signals. The average distance between the maxima observed in the echo amplitude, determined by counting the number of oscillations as the receiver was tuned over a controlled frequency range, was found to be $2\pi/\tau_{12}$ (Ref. 74).

The depth of the oscillations at the selected value $\tau_{12} = 10 \mu\text{s}$ is of course small, since the passband (1 MHz) of the particular receiver used includes a large number of these maxima of the function $g(\Delta\omega')$. However, if the free-induction signal after the second rf pulse has not yet decayed by the time at which the echo is formed ($\tau_{12} = 8 \mu\text{s}$), the depth of the recorded oscillations increased to 100% (Ref. 39). This effect was explained in Ref. 36.

Direct measurements of the spectrum of the frequency-modulated echo have also been carried out successfully by a parametric-echo method²² (Fig. 16).

Another experiment confirming the frequency-modulation nature of the formation of the echo signal in a system

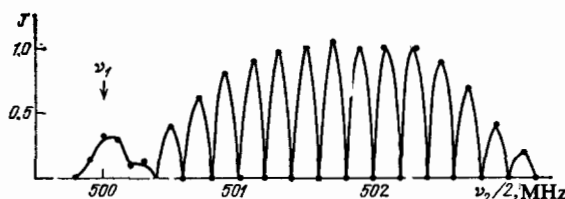


FIG. 16. Amplitude of the parametric echo as a function of the frequency of the parametric pulse, ν_r , under conditions corresponding to the formation of the single-pulse echo.²²

with a dynamic frequency shift is a study of the dependence of the echo intensity on the delay time between the pulses, τ_{12} . While in the Hahn mechanism for the formation of an echo the dependence of the echo intensity on this delay time is determined exclusively by relaxation processes [see (38) and (42)], the intensity of the frequency-modulation echo is a rather complicated function of τ_{12} [see (55) and (56)].⁹⁾ In particular, at small amplitudes of the rf pulses, $s \ll 1$ [see (56)], the amplitude of the frequency-modulation echo should initially increase with increasing delay time and then reach a maximum at $\tau_{12} = T_2/2$:

$$U_{\text{echo}}(\tau) = c\eta n_0 \omega_n \alpha \beta^2 \omega_p \tau_{12} e^{-2\tau_{12}/T_2}. \quad (57)$$

The physical nature of this effect can be described by saying that the second rf pulse causes frequency modulation of the NMR line, (45) (Fig. 5). For the formation of a frequency-modulated echo, however, the frequency redistribution of the nuclear spins must give rise to a redistribution of the spin precession phases, and this process would require some time. During the initial part of the increase in τ_{12} (at $\tau_{12} \ll T_2$), therefore, the effectiveness of the frequency-modulation mechanism and correspondingly the amplitude of the frequency-modulated echo should increase linearly. At $\tau_{12} > T_2/2$, however, relaxation processes which exponentially reduce the amplitude of the frequency modulation will be more important.

For a long time, experiments revealed only a monotonic decrease in the intensity of the frequency-modulated echo with an increase in the delay time; this situation was apparently a consequence of the short transverse relaxation times T_2 for the particular samples.^{32-34,37,38} A CsMnF_3 single crystal with an anomalously long transverse relaxation time, $T_2 \sim 140 \mu\text{s}$, was selected in an effort to observe the effect under discussion here. The experiments on this crystal revealed that two regions could be distinguished in the dependence of the echo intensity on the delay time (Fig. 17): a region of small delay times, in which the signal decreases

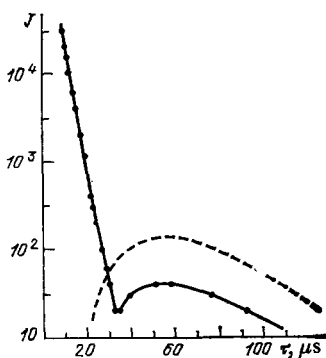


FIG. 17. Intensity of the two-pulse echo of Mn^{55} in CsMnF_3 as a function of the time interval (τ) between the exciting rf pulses at $T = 2.0 \text{ K}$ (Ref. 75). $\nu_{\text{NMR}} = 639 \text{ MHz}$, $\omega_p/2\pi = 27 \text{ MHz}$, $\tau_2 = 18 \mu\text{s}$. The dashed curve is theoretical, drawn from Eq. (57).

⁹⁾ Furthermore, a nonlinearity of the motion of the nuclear spins and a nonuniformity of the rf field may give rise to some additional, exponentially decaying factors in the τ_{12} dependence of the intensity of the frequency-modulated echo.^{29,64} In this case the measured relaxation time would be much shorter than the true time.

monotonically,¹⁰⁾ and a region of long delay times, in which the dependence is that characteristic of a frequency-modulation echo.⁷⁵ The position of the maximum on this dependence at various temperatures and also the shape of the curves and the relative intensities of the maxima agree well with the theory of the frequency-modulated echo [see (57)].

One of the advantages of the spin-echo method is that the longitudinal (T_1) and transverse (T_2) relaxation times can be measured directly from the dependence of the echo intensity on the time interval between the corresponding pulses. The results show that in the case of the frequency-modulated echo one should use caution in determining the relaxation times from these curves. The use of the stimulated frequency-modulated echo to determine the longitudinal relaxation time T_1 is complicated even further by the nontrivial properties of this echo. The stimulated frequency-modulated echo, in contrast with the two-pulse echo, is observed only with a comparatively small dynamic frequency shift.^{37,42} In MnCO_3 , for example, the stimulated frequency-modulated echo is observed only over the frequency range 615–630 MHz at $\omega_{n0}/2\pi = 640 \text{ MHz}$, while the two-pulse echo reaches a maximum in the region 580–620 MHz.

To conclude this subsection of the review we consider two experimental results associated with pulling of the precession frequency of nuclear spins by an rf field.

An intensification of the two-pulse frequency-modulated echo was observed in Ref. 32 when preliminary pulse was applied at a power level much higher than that of the exciting rf pulses. This effect was observed in MnO under conditions of pronounced broadening of the NMR line. The power level of the rf pulses was such that for most of the isochromatic groupings the trajectories of their motions during the pulse did not satisfy the linearity condition [see (25)]. In this experiment the preliminary pulse apparently resulted in pulling of the spin system by the rf field, with the result that the spin precession frequencies changed to the frequency of the preliminary pulse, the inhomogeneous broadening of the NMR line decreased, and the conditions for the formation of an echo signal were improved. The processes by which a spin system is pulled by an rf field had been studied previously by cw methods.^{20,50} Other experiments³⁸ had also been carried out in which it was shown that the effect of the preliminary pulse intensifies when its frequency is slightly above the frequency of the exciting pulses. There is a more effective narrowing of the NMR line in this case.

Another experimental effect, also associated with the adjustment of the spin precession frequency to the frequency of the rf pulse, is the "pulled-echo effect" discovered in Ref. 37. This pulled echo is the signal formed at the frequency of the exciting rf pulses, which differs from the frequency of the unperturbed NMR line. That difference between ω_n and ω_{rf} at which the pulled-echo signal arises depends on the power

¹⁰⁾ A detailed analysis of the results shows that at short delay times the echo is not formed by the frequency-modulation mechanism discussed above. At this point we cannot explain this echo on the basis of the present understanding of the dynamics of the motion of nuclear magnetization in spin systems with a dynamic frequency shift.

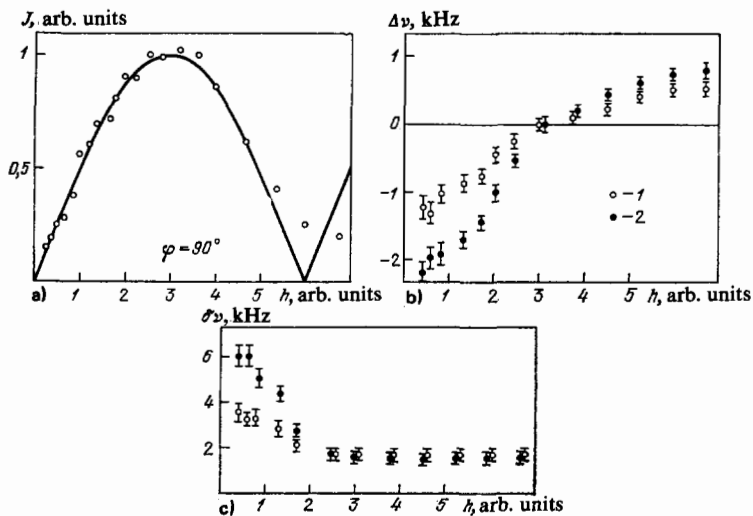


FIG. 18. Characteristics of the free-induction signal as functions of the amplitude of the rf field in FeBO_3 (Ref. 46). a—Dependence of the amplitude of the induction signal at $T = 4.2\text{ K}$; b—dependence of the frequency shift $\Delta\nu$ of the induction signal at $T = 4.2\text{ K}$ (1) and $T = 2.0\text{ K}$ (2); c—dependence of the broadening of the NMR line at the same temperatures.

level of the rf pulses. Studies of this effect showed that the rf pulse causes the precession frequency of the spins forming the echo signal to shift from ω_n to ω_{rf} ; i.e., the spin system is pulled. Although the mechanism for the formation of the pulled echo has not yet been determined, the dependence of its frequency on the amplitude of the first rf pulse suggests that the spins are driven by the rf field along trajectories near an aperiodic trajectory (Fig. 2c).

Together, these experimental results confirm qualitatively, and in some cases quantitatively, the theory for the motion of nuclear magnetization in spin systems with a dynamic frequency shift under the influence of a resonant rf field. These results also agree well with the theory for the mechanism for the formation of the frequency-modulated echo.

In the final subsection of this review we will briefly discuss the pulsed responses of spin systems with a small dynamic frequency shift and the particular features of the dynamic frequency shift for nuclei at domain walls in magnetic crystals.

9. Spin systems with a small dynamic NMR frequency shift

We have already outlined the basic experimental results from studies of nuclear spin systems with a large dynamic shift of the NMR frequency, in which case the shift is considerably greater than the width of the NMR line ($\omega_p \gg 1/T_2^*$). The theory discussed earlier also applies only in the case of a large shift. Equations (13) are valid under the condition that the nuclear spins precess with an identical phase over distances of the order of the range of the Suhl-Nakamura interaction. Analysis shows that in the case of a large dynamic shift of the NMR frequency this condition clearly holds.⁷⁶ In the opposite case of a small shift ($\omega_p \approx 1/T_2^*$) we can expect that the loss of phase coherence of the transverse nuclear magnetization will disrupt the dynamic frequency shift.¹¹⁾

¹¹⁾Tsifrinovich and Krasnov⁷⁷ have attempted to take into account quantitatively the effect of the dynamic frequency shift on the microinhomogeneous broadening for a NMR line of Lorentzian shape. Their results, however, are in poor agreement with the experimental results available, apparently because of the particular broadening shape chosen.

Studies of NMR with a small dynamic frequency shift are interesting for determining the nature of the transition from the dynamics of an ordinary paramagnetic nuclear system to the dynamics of a coupled electron-nuclear system with a dynamic shift of the NMR frequency.

A study of the properties of the two-pulse spin echo and of the free-induction signal of Fe^{57} nuclei in slightly ferromagnetic FeBO_3 at temperatures $T = 2\text{--}4.2\text{ K}$ was reported in Ref. 46. Under these conditions, the expected dynamic frequency shifts ($\omega_p \sim 5/T$ kHz) is of the order of the inhomogeneous broadening of the NMR line.¹²⁾

Direct measurements of the frequency of the free-induction signal (Fig. 18b) and the temperature dependence of the NMR frequency revealed that the dynamic frequency shift observed experimentally is essentially the same as the theoretical shift.¹³⁾

One of the interesting experimental results is the dependence of the width of the NMR line (determined from the decay rate of the free-induction signal) on the angle (φ) through which the nuclear magnetization is deflected from its equilibrium direction (Figs. 18a and 18c). It turns out that the width of the NMR line decreases significantly with increasing φ . At $\varphi > 90^\circ$, however, the line width becomes independent of the amplitude of the rf field. The maximum change in the width of the NMR line, $\Delta\nu_{\text{max}}$, turns out to be approximately equal to the dynamic frequency shift and has the same temperature dependence ($\Delta\nu_{\text{max}} \sim 1/T$). Further experiments showed that the quantity $\Delta\nu_{\text{max}}$ is proportional to the projection of the nuclear magnetization onto the hyperfine field which prevails at the time at which the rf pulse is applied. It has thus been shown experimentally that the dynamic frequency shift in FeBO_3 gives rise to a significant broadening of the NMR line.

¹²⁾These experiments were carried out on a Bruker SXP-4-100 pulsed spectrometer in the Vihuri Physics Laboratory at the University of Turku, Finland.

¹³⁾The dynamic frequency shift in FeBO_3 enriched to 85% in the isotope Fe^{57} (the natural abundance is 2.2%) was measured at $T = 4.2\text{ K}$ in Ref. 78. The experimental shift ($\sim 10\text{ kHz}$), however, turned out to be several times smaller than the theoretical shift.

Interestingly, at low amplitudes of the rf field (in the region of the anomalous broadening of the NMR line; see Fig. 18c) the two-pulse spin echo is not observed. When there is a short delay between the rf pulses, however, a structural feature is found on the induction signal; at the time $t = 2\tau_{12}$; the height of this feature reaches a maximum when the phases of the rf pulses differ by 90° .

It was concluded in Ref. 46 from an analysis of the results obtained that the observed broadening of the NMR line is homogeneous and that the structural feature which appears on the free-induction signal after the second pulse is analogous to the "solid echo" which is formed in spin systems with a homogeneous broadening of the magnetic-resonance line.⁷⁹

10. Dynamic NMR frequency shift of nuclei in domain walls

Most of the theoretical and experimental results described above are of the dynamic frequency shift of nuclei in domains. For nuclear spins in domain walls the gain η is usually much larger than that for nuclei in the domains themselves and can reach $\eta = 10^3-10^5$. On this basis we might expect that the dynamic frequency shift would be particularly large for nuclei in domain walls.^{19,80,81}

The situation is considerably more complicated in this case, however, because for nuclei in domain walls there is usually a large spread in the resonant frequency and also in the gain because of the angular distribution of the spins in a wall.⁸²

Another distinctive feature of these dynamic effects is the approximate equality of the resonant frequencies of nuclear spins and domain walls. Under these conditions the alternating magnetic field produced by the electron system at the nuclei in a domain wall will lag in phase behind the external agent, with important consequences for the nature of the dynamic effects.

Experiments on the dynamic frequency shift for nuclei in domain walls have been carried out at $T = 1.7$ K for the spin system of Mn^{55} nuclei in manganese ferrite,^{39,44,83} $MnFe_2O_4$.

Under these conditions the dynamic shift of the NMR frequency is $|\omega_p/2\pi| \geq 0.4-0.6$ MHz, and the sign of the shift is opposite to that for the shift for nuclei in domains of slightly anisotropic antiferromagnetic materials such as $MnCO_3$. In the present case, the dynamic shift of the NMR frequency increases the NMR frequency of the nuclei of interest as the temperature is lowered. This result indicates that the frequencies of the domain walls are lower than those of the Mn^{55} nuclei in the walls, in accordance with the data from magnetic measurements.⁸⁴

The properties of the spin echo from nuclei which lie in domain walls in $MnFe_2O_4$ and which exhibit a dynamic frequency shift (the so-called additional echo) are quite different from those of the other known types of echos⁸⁵ (Fig. 19). Many of the properties have yet to be fully explained because of the complexities of the mathematical description (among these properties are the width of the echo, the optimum conditions for observing it, the dependence of the time at which it appears on the amplitude of the rf pulses, the anomalous

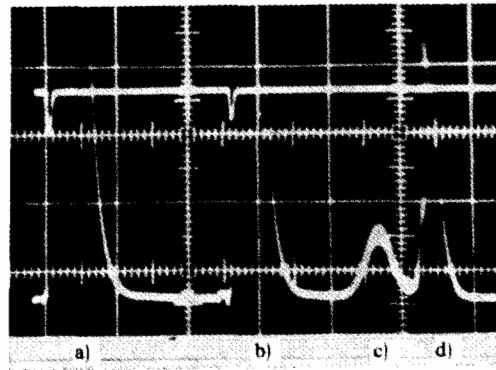


FIG. 19. Additional (c) and fundamental (d) signals of the nuclear echo of Mn^{55} in $MnFe_2O_4$ after two exciting rf pulses. The upper trace is the signal from a wave meter, to show the positions of the rf pulses ($\nu_{rf} = 585.7$ MHz, $\tau_{12} = 27 \mu s$, $T = 1.7$ K).

properties of the stimulated echo, and the instability of the echo amplitude). An attempt to find a qualitative explanation for some of the effects was made in Ref. 86.

A dynamic frequency shift for nuclei in domain walls was also observed recently in europium iron garnet, $Eu_3Fe_5O_{12}$, in a study of the properties of the two-pulse echo of Eu^{151} nuclei.⁴⁵

IV. CONCLUSION

It is fair to say that the basic results of the research by pulsed methods on magnetically ordered crystals exhibiting a dynamic NMR frequency shift are the discovery of and the proof of the effectiveness of two new mechanisms for the formation of echos: the frequency-modulation echo, whose properties have largely been the subject of this review, and the parametric echo.²²

The body of experimental information presently available on the frequency-modulated echo can be described quite well by the existing theory, although several results have yet to be explained. In particular, no theoretical explanation has been found for the properties of the stimulated echo, the pulled-echo effect,³⁷ and several effects associated with the time at which the echos appear.^{60,65}

Active research continues on the appearance of the dynamic frequency shift in spin systems and the particular features of the shift and the pulsed resonances of the spin system of nuclei in a domain wall.

We thus have a group of questions whose understanding will require further development of the theory of nuclear magnetic resonance under conditions involving a dynamic frequency shift.

We will conclude with a list of some interesting results on spin systems with a dynamic frequency shift which we have not discussed above.

A dynamic shift of the NMR frequency has been observed in an antiferromagnetic material with a large gap in the antiferromagnetic-resonance spectrum of MnF_2 near a spin flop.⁸⁷

It has been shown that when an rf field is applied at frequencies near the resonant frequencies a spin system of

nuclei with a dynamic frequency shift can be in two states, with different values of m_z (Ref. 89).

The dynamic frequency shift has been studied theoretically for the case in which the NMR and ferromagnetic-resonance frequencies are equal. It has been shown that there is an effective new mechanism for nuclear relaxation: "electron-nuclear magnetic relaxation."⁹⁰

Some distinctive features have been found in the frequency-modulation mechanism for echo formation at high amplitudes of the rf pulses⁹¹ ($\omega_1 \gg \omega_p$).

Finally, we would like to point out that, although effects with a dynamic frequency shift in nuclear systems have been studied in comparatively few materials, the trend toward lower temperatures in modern physics will make the effect a typical one in the resonances of magnetic crystals. Furthermore, the approach developed here may be useful for analyzing other systems, e.g., superfluid He³ (Ref. 92), which exhibits a nonlinearity of the type discussed here.

There are also echo effects which do not involve spins, e.g., the so-called phonon or electroacoustic echo,⁹³ many aspects of which can be described by the same methods as in the present review.

We wish to thank L. L. Buishvili, V. V. Dmitriev, V. V. Moskalev, A. A. Petrov, and A. V. Ivanov for a discussion of the manuscript and for many useful comments.

¹E. K. Zavoiskii, J. Phys. USSR **8**, 377 (1944).

²E. M. Purcell, H. C. Torrey, and R. V. Pound, Phys. Rev. **69**, 37 (1946).

³F. Bloch, W. W. Hansen, and M. Packard, Phys. Rev. **69**, 127 (1946).

⁴E. L. Hahn, Phys. Rev. **80**, 580 (1950).

⁵N. J. Poulis and G. E. Hardemann, Physica (Utrecht) **18**, 201 (1952); **19**, 391 (1953).

⁶A. C. Gossard and A. M. Portis, Phys. Rev. Lett. **3**, 164 (1959).

⁷V. Jaccarino, in: Magnetism, Vol. 2A, Academic Press, New York, 1965, p. 307.

⁸A. M. Portis and R. H. Lindquist, in: Magnetism, Vol. 2A, Academic Press, New York, 1965, p. 357.

⁹E. A. Turov and M. P. Petrov, Yaderniy magnitnyy rezonans v ferro-antiferromagnetikakh, Nauka, Moscow, 1969. (Engl. Transl.) Nuclear Magnetic Resonance in Ferro- and Antiferromagnets, Israel Program for Scientific Translations, Jerusalem; Wiley, New York (1972).

¹⁰M. P. Petrov and E. A. Turov, Appl. Spectrosc. Rev. **5**(2), 265 (1971).

¹¹E. Dorman, Festkörperprobleme **12**, 487 (1972).

¹²T. J. Burch and J. I. Budnik, Mag. Res. Rev. **2**, 247 (1973).

¹³M. P. Petrov, in: Fizika magnitnykh dielektrikov (Physics of Magnetic Dielectrics), Nauka, Leningrad, 1974, p. 177.

¹⁴V. A. Golenioshev-Kutuzov, in: Problemy magnitnogo rezonansa (Problems of Magnetic Resonance), Nauka, Moscow, 1978, p. 98.

¹⁵E. A. Turov and M. I. Kurkin, in: Problemy magnitnogo rezonansa (Problems of Magnetic Resonance), Nauka, Moscow, 1978, p. 271.

¹⁶M. P. Petrov, V. P. Chekmarev, and A. P. Paugurt, in: Problemy magnitnogo rezonansa (Problems of Magnetic Resonance), Nauka, Moscow, 1978, p. 289.

¹⁷Yu. M. Bun'kov and B. S. Dumesh, in: Problemy magnitnogo rezonansa (Problems of Magnetic Resonance), Nauka, Moscow, 1978, p. 310.

¹⁸V. A. Tulin, Fiz. Nizk. Temp. **5**, 965 (1979) [Sov. J. Low Temp. Phys. **5**, 455 (1979)].

¹⁹P. G. De Gennes, P. A. Pinkus, F. Hartmann-Boutron, and J. M. Winter, Phys. Rev. **129**, 1105 (1963).

²⁰V. A. Tulin and A. S. Borovik-Romanov, Pis'ma Zh. Eksp. Teor. Fiz. **1**, 18 (1965) [sic]; V. A. Tulin, Zh. Eksp. Teor. Fiz. **55**, 831 (1968) [Sov. Phys. JETP **28**, 431 (1979)]; V. Minkiewicz and A. Nakamura, Phys. Rev. **143**, 361 (1966); K. Lee, A. M. Portis, and L. S. Witt, Phys. Rev. **132**, 144 (1963); V. Minkiewicz and A. Nakamura, Phys. Rev. **143**, 356 (1966); D. Shaltiel, Phys. Rev. **142**, 300 (1966).

²¹A. J. Heeger, A. M. Portis, D. T. Teaney, and C. L. Witt, Phys. Rev. Lett. **7**, 308 (1961).

²²Yu. M. Bun'kov, Pis'ma Zh. Eksp. Teor. Fiz. **23**, 271 (1976) [JETP Lett.

23, 244 (1976)]; Yu. M. Bun'kov and S. O. Gladkov, Zh. Eksp. Teor. Fiz. **73**, 2181 (1977) [Sov. Phys. JETP **46**, 1141 (1977)].

²³A. Abragam, The Principles of Nuclear Magnetism, Oxford Univ. Press, London, 1961 (Russ. Transl. IL, Moscow, 1963).

²⁴S. V. Vonsovskii, Magnetizm, Nauka, Moscow, 1971 [Engl. Transl. (Magnetism), Halsted, New York (1975)].

²⁵A. S. Borovik-Romanov, in: Itogi nauki. Fiz.-matem. nauki. (Scientific Progress. Physicomathematical Sciences), Vol. 4, Izd. Akad. Nauk SSSR, Moscow, 1962, p. 7.

²⁶H. Suhl, Phys. Rev. **109**, 606 (1958); T. Nakamura, Prog. Theor. Phys. **20**, 542 (1958).

²⁷E. A. Turov, M. I. Kurkin, and V. V. Nikolaev, Zh. Eksp. Teor. Fiz. **64**, 283 (1973) [Sov. Phys. JETP **37**, 147 (1973)].

²⁸A. P. Vereshchagina and V. V. Moskalev, in: Yaderniy magnitnyy rezonans (Nuclear Magnetic Resonance), Izd. Leningr. Univ., Leningrad, 1974, No. 5, p. 38.

²⁹M. I. Kurkin and V. V. Nikolaev, Fiz. Met. Metalloved. **38**, 957 (1974).

³⁰K. M. Salikhov, A. G. Semenov, and Yu. D. Tsvetkov, Elektronnoe spinovoe ékho i ego primeneniye (The Electron Spin Echo and Its Applications), Nauka, Novosibirsk, 1976.

³¹R. W. Gould, Phys. Lett. **A29**, 347 (1969).

³²P. M. Richards, C. R. Christensen, B. D. Guenther, and A. C. Daniel, Phys. Rev. **B4**, 2216 (1971); C. R. Christensen, B. D. Guenther, and A. C. Daniel, Bull. Am. Phys. Soc. **14**, 1185 (1969).

³³M. P. Petrov, G. A. Smolenskii, A. A. Petrov, and S. I. Stepanov, Fiz. Tverd. Tela (Leningrad) **15**, 184 (1973) [Sov. Phys. Solid State **15**, 126 (1973)].

³⁴A. A. Petrov, Candidate's Dissertation, A. F. Ioffe Physicotechnical Institute, Academy of Sciences of the USSR, Leningrad, 1975.

³⁵S. A. Zel'dovich and A. R. Kessel', Fiz. Tverd. Tela (Leningrad) **17**, 3137 (1975) [Sov. Phys. Solid State **17**, 2075 (1975)].

³⁶V. P. Chekmarev and M. P. Petrov, Zh. Eksp. Teor. Fiz. **71**, 377 (1976) [Sov. Phys. JETP **44**, 197 (1976)].

³⁷Yu. M. Bun'kov and B. S. Dumesh, Zh. Eksp. Teor. Fiz. **68**, 1161 (1975) [Sov. Phys. JETP **41**, 576 (1975)].

³⁸B. S. Dumesh, Candidate's Dissertation, Institute of Physical Problems, Academy of Sciences of USSR, Moscow, 1975.

³⁹V. P. Chekmarev, Candidate's Dissertation, A. F. Ioffe Physico-technical Institute, Academy of Sciences of the USSR, Leningrad, 1978.

⁴⁰Yu. M. Bun'kov, Candidate's Dissertation, Institute of Physical Problems, Academy of Sciences of the USSR, Moscow, 1979.

⁴¹B. S. Dumesh, Pis'ma Zh. Eksp. Teor. Fiz. **14**, 511 (1971) [JETP Lett. **14**, 350 (1971)].

⁴²A. A. Petrov, M. P. Petrov, G. A. Smolenskii, and P. P. Syrnikov, Pis'ma Zh. Eksp. Teor. Fiz. **14**, 514 (1971) [JETP Lett. **14**, 353 (1971)].

⁴³B. S. Dumesh, Pis'ma Zh. Eksp. Teor. Fiz. **23**, 17 (1976) [JETP Lett. **23**, 14 (1976)].

⁴⁴V. P. Chekmarev, M. P. Petrov, A. A. Petrov, and V. V. Kulikov, Pis'ma Zh. Eksp. Teor. Fiz. **25**, 181 (1977) [JETP Lett. **25**, 165 (1977)].

⁴⁵V. I. Belotitskii and V. P. Chekmarev, in: Radiospektroskopiya (Rf Spectroscopy), Perm', 1980, p. 36.

⁴⁶Yu. M. Bun'kov, M. Punkinen, and E. E. Yulinen, Zh. Eksp. Teor. Fiz. **74**, 1170 (1978) [Sov. Phys. JETP **47**, 615 (1978)].

⁴⁷A. M. Pogorelyi and V. V. Kotov, Zh. Eksp. Teor. Fiz. **79**, 2200 (1980) [sic].

⁴⁸L. B. Welsh, Phys. Rev. **156**, 370 (1967).

⁴⁹A. S. Borovik-Romanov, N. M. Kreines, and L. A. Prozorova, Zh. Eksp. Teor. Fiz. **45**, 64 (1970) [sic].

⁵⁰V. A. Tulin, Zh. Eksp. Teor. Fiz. **58**, 1265 (1970) [Sov. Phys. JETP **31**, 680 (1970)].

⁵¹A. J. Heeger and D. T. Teaney, J. Appl. Phys. **35**, 846 (1964).

⁵²W. J. Ince, Phys. Rev. **184**, 574 (1969).

⁵³A. N. Andrienko and L. A. Prozorova, Zh. Eksp. Teor. Fiz. **74**, 1527 (1977) [sic].

⁵⁴V. S. Mandel', V. D. Voronkov, and D. E. Gromzin, Zh. Eksp. Teor. Fiz. **63**, 993 (1972) [Sov. Phys. JETP **36**, 521 (1972)].

⁵⁵A. R. King, V. Jaccarino, and S. M. Rezende, Phys. Rev. Lett. **37**, 553 (1976).

⁵⁶L. V. Velikov, A. S. Prokhorov, E. G. Rudashevskii, and V. N. Seleznev, Zh. Eksp. Teor. Fiz. **66**, 1847 (1974) [Sov. Phys. JETP **39**, 909 (1974)].

⁵⁷D. D. Osheroff and L. R. Corruccini, Phys. Lett. **A51**, 447 (1975).

⁵⁸A. I. Ahonen, M. Krusius, and M. A. Paalanen, J. Low. Temp. Phys. **25**, 421 (1976).

⁵⁹O. Avenel, P. Berglund, M. Bernier, and J. M. Delrieu, in: Proceedings of the Nineteenth Congress AMPERE, Heidelberg, 1976, p. 123.

⁶⁰A. S. Borovik-Romanov and B. S. Dumesh, in: Proceedings of the Seventeenth Congress AMPERE, North-Holland, Amsterdam, 1973, p. 470.

- ⁶¹Yu. M. Bun'kov, V. S. Lutovinov, and A. A. Monakhov, *Zh. Eksp. Teor. Fiz.* **80**, 1449 (1981) [*Sov. Phys. JETP* **53**, 742 (1981)].
- ⁶²H. Pfeifer, *Ann. Phys. (Leipzig)* **17**, 23 (1955).
- ⁶³A. S. Borovik-Romanov, Yu. M. Bunkov, B. S. Dumesh, and V. A. Tulin, in: *Proceedings of the Eighteenth Congress AMPERE, Nottingham, 1974*, p. 5.
- ⁶⁴M. I. Kurkin and E. A. Turov, *Fiz. Met. Metalloved.* **40**, 714 (1975).
- ⁶⁵A. A. Petrov, M. P. Petrov, and V. P. Chekmarev, *Fiz. Tverd. Tela (Leningrad)* **17**, 2640 (1975) [*Sov. Phys. Solid State* **17**, 1755 (1975)].
- ⁶⁶Yu. M. Bun'kov, B. S. Dumesh, and M. I. Kurkin, *Pis'ma Zh. Eksp. Teor. Fiz.* **19**, 216 (1974) [*JETP Lett.* **19**, 132 (1974)].
- ⁶⁷E. L. Bloom, *Phys. Rev.* **98**, 1105 (1955); B. M. Stearns, *AIP Conf. Proc.* **10**, 1644 (1972).
- ⁶⁸V. P. Chekmarev, M. I. Kurkin, and S. I. Goloshchapov, *Zh. Eksp. Teor. Fiz.* **76**, 1675 (1979) [*Sov. Phys. JETP.* **49**, 851 (1979)].
- ⁶⁹V. P. Chekmarev and M. I. Kurkin, *Fiz. Tverd. Tela (Leningrad)* **18**, 1954 (1976) [*Sov. Phys. Solid State* **18**, 1137 (1976)].
- ⁷⁰V. P. Chekmarev and G. I. Mamniashvili, *Fiz. Met. Metalloved.* **51**, 685 (1981).
- ⁷¹M. I. Kurkin and V. V. Serikov, *Fiz. Tverd. Tela (Leningrad)* **16**, 1177 (1974) [*Sov. Phys. Solid State* **16**, 755 (1975)].
- ⁷²M. P. Petrov, A. P. Paugurt, G. A. Smolenskiĭ, and M. K. Chizov, *Izv. Akad. Nauk SSSR, Ser. Fiz.* **36**, 1472 (1972); M. P. Petrov, V. V. Moskalev, and G. A. Smolenskiĭ, *Pis'ma Zh. Eksp. Teor. Fiz.* **15**, 132 (1972) [*JETP Lett.* **15**, 91 (1972)]. C. W. Searle, J. Davis, A. Hirai, and K. Fukuda, *Phys. Rev. Lett.* **27**, 1380 (1971).
- ⁷³W. B. Mims, *Phys. Rev.* **141**, 499 (1966).
- ⁷⁴V. P. Chekmarev, M. P. Petrov, and A. A. Petrov, *Fiz. Tverd. Tela (Leningrad)* **17**, 1822 (1975) [*Sov. Phys. Solid State* **17**, 1193 (1975)]; M. P. Petrov, V. P. Chekmarev, and A. A. Petrov, *Physica (Utrecht)* **B86**, 1305 (1977).
- ⁷⁵Yu. M. Bun'kov and V. V. Dmitriev, *Zh. Eksp. Teor. Fiz.* **80**, 2363 (1981) [*Sov. Phys. JETP* **53**, 1237 (1981)].
- ⁷⁶M. I. Kurkin, Doctoral Dissertation, Institute of Metal Physics, Ural Scientific Center of the Academy of Sciences of the USSR, Sverdlovsk, 1979.
- ⁷⁷V. I. Tsifrinovich and I. V. Krasnov, *Zh. Eksp. Teor. Fiz.* **78**, 1760 (1980) [*Sov. Phys. JETP* **51**, 883 (1980)].
- ⁷⁸M. P. Petrov and V. R. Korneev, in: *Proceedings of the Twentieth Congress AMPERE, Tallin, 1978*, p. 357.
- ⁷⁹P. Mansfield, *Phys. Rev.* **A137**, 961 (1965).
- ⁸⁰M. P. Petrov and V. V. Moskalev, *Fiz. Tverd. Tela (Leningrad)* **15**, 2537 (1973) [*Sov. Phys. Solid State* **15**, 1689 (1973)].
- ⁸¹M. A. Shamsutdinov and M. M. Farztdinov, *Fiz. Tverd. Tela (Leningrad)* **17**, 3306 (1975) [*Sov. Phys. Solid State* **17**, 2169 (1975)].
- ⁸²E. A. Turov, A. P. Tankeev, and M. I. Kurkin, *Fiz. Met. Metalloved.* **28**, 385 (1969); **29**, 747 (1970).
- ⁸³V. P. Chekmarev, M. P. Petrov, and A. A. Petrov, *Fiz. Tverd. Tela (Leningrad)* **21**, 1095 (1979) [*Sov. Phys. Solid State* **21**, 636 (1979)].
- ⁸⁴S. E. Harrison, C. J. Kriesman, and Q. Q. Pollack, *Phys. Rev.* **110**, 844 (1958).
- ⁸⁵V. P. Chekmarev, M. P. Petrov, and A. A. Petrov, *Fiz. Tverd. Tela (Leningrad)* **21**, 2641 (1979) [*Sov. Phys. Solid State* **21**, 1519 (1979)].
- ⁸⁶V. P. Chekmarev, V. I. Belotitskiĭ, and G. I. Mamniashvili, *Fiz. Tverd. Tela (Leningrad)* **24**, 222 (1982) [*Sov. Phys. Solid State* **24**, 123 (1982)].
- ⁸⁷A. R. King, V. Jaccarino, and S. M. Rezende, *Phys. Rev. Lett.* **37**, 533 (1976).
- ⁸⁸B. S. Dumesh, *Pis'ma Zh. Eksp. Teor. Fiz.* **24**, 167 (1976) [*JETP Lett.* **24**, 145 (1976)].
- ⁸⁹M. I. Kurkin, *Pis'ma Zh. Eksp. Teor. Fiz.* **28**, 675 (1978) [*JETP Lett.* **28**, 628 (1978)].
- ⁹⁰V. I. Tsifrinovich and V. A. Ignatchenko, *Zh. Eksp. Teor. Fiz.* **72**, 803 (1977) [*Sov. Phys. JETP* **45**, 419 (1977)].
- ⁹¹M. G. Menabde, *Fiz. Tverd. Tela (Leningrad)* **22**, 135 (1980) [*Sov. Phys. Solid State* **22**, 77 (1980)].
- ⁹²M. Bernier and J. H. Delrieu, Cited in Ref. 59, p. 127.
- ⁹³S. N. Popov and N. M. Kraĭnik, *Fiz. Tverd. Tela (Leningrad)* **12**, 3022 (1970) [*Sov. Phys. Solid State* **12**, 2440 (1970)]; A. R. Kessel', I. A. Safin, and A. M. Gol'dman, *Fiz. Tverd. Tela (Leningrad)* **12**, 3070 (1970) [*Sov. Phys. Solid State* **12**, 2488 (1970)].

Translated by Dave Parsons